

A Tensor-EM Method for Large-Scale Latent Class Analysis with Clustering Consistency

Zhenghao Zeng¹, Yuqi Gu², and Gongjun Xu³

¹Carnegie Mellon University

²Duke University

³University of Michigan, Ann Arbor

Abstract

Latent class models are powerful statistical modeling tools widely used in psychological, behavioral, and social sciences. In the modern era of data science, researchers often have access to response data collected from large-scale surveys or assessments, featuring many items (large J) and many subjects (large N). This is in contrary to the traditional regime with fixed J and large N . To analyze such large-scale data, it is important to develop methods that are both computationally efficient and theoretically valid. In terms of computation, the conventional EM algorithm for latent class models tends to have a slow algorithmic convergence rate for large-scale data and may converge to some local optima instead of the maximum likelihood estimator (MLE). Motivated by this, we introduce the tensor decomposition perspective into latent class analysis. Methodologically, we propose to use a moment-based tensor power method in the first step, and then use the obtained estimators as initialization for the EM algorithm in the second step. Theoretically, we establish the clustering consistency of the MLE in assigning subjects into latent classes when N and J both go to infinity. Simulation studies suggest that the proposed tensor-EM pipeline enjoys both good accuracy and computational efficiency for large-scale data. We also apply the proposed method to a personality dataset as an illustration.

Keywords: Large-scale latent class analysis; Tensor decomposition; Tensor power method; EM algorithm; Clustering consistency.

1 Introduction

Latent class models (LCMs) (Lazarsfeld and Henry, 1968; Goodman, 1974) are powerful statistical modeling tools widely used in psychological, behavioral, and social sciences. LCMs use a categorical latent variable to model the unobserved heterogeneity of multivariate categorical data and identify meaningful latent subgroups of subjects. LCMs have seen broad applications in a variety of scientific fields, including psychology and psychiatry (Bucholz et al., 2000; Keel et al., 2004), sociology and organizational research (Wang and Hanges, 2011), and biomedical and epidemiological studies (Bandein-Roche et al., 1997; Dean and Raftery, 2010). There are also various extensions and generalizations building upon LCMs, including LCMs with covariates or distal outcomes (Vermunt, 2010; Lanza and Rhoades, 2013), longitudinal LCMs and latent transition analysis (Dunn et al., 2006; Collins and Lanza, 2009), and also restricted LCMs known as diagnostic classification models that involve multiple categorical latent variables (Rupp and Templin, 2008; Xu, 2017; von Davier and Lee, 2019). For general introductions and applications of LCMs, see Hagenaars and McCutcheon (2002) and Collins and Lanza (2009).

In this paper, we focus on LCMs with binary responses for large-scale data, which are typically collected in modern educational assessments (correct/wrong responses) and psychological or social science surveys (yes/no responses). Such data are characterized by many test takers with large N and also many items with large J . This is in contrary to the traditional regime with large N and fixed J , a relatively well understood setting. Such a large scope of data poses challenges to classical statistical analysis methods and calls for new developments for LCMs. In the following, we summarize the two main questions motivating our study.

The first question of large-scale latent class analysis is how to perform computation efficiently. A conventional estimation method is the Expectation-Maximization (EM; Dempster et al., 1977) algorithm to maximize the marginal likelihood. EM algorithms have two potential drawbacks, the slow algorithmic convergence rate in high dimensions and a tendency to converge to some local optima when the initial values are poorly chosen (Balakrishnan et al., 2017). In practice, researchers often run EM with many random initializations and select the one that gives the largest log-likelihood value. This procedure can be very time-consuming, especially for large-scale data. It

is thus desirable to develop more efficient computational tools for large-scale latent class analysis. Motivated by this, we introduce the tensor decomposition perspective into latent class analysis.

There has been active research on tensor decompositions since they were introduced in [Hitchcock \(1927\)](#). The concept of tensors appeared in the literature of psychometrics dating back to 1960s-1970s ([Tucker, 1964, 1966](#); [Harshman, 1970](#); [Kruskal, 1976](#)). The interest of tensor decompositions has expanded to other areas, including chemometrics ([Smilde et al., 2005](#)), signal processing ([De Lathauwer and De Moor, 1998](#)), and data mining ([McCullagh, 2018](#)). In particular, tensor methods have also been used in learning latent variable models ([Anandkumar et al., 2012](#); [Hsu and Kakade, 2013](#); [Anandkumar et al., 2014](#)). [Anandkumar et al. \(2014\)](#) summarized the common structures in several different latent variable models and used tensor power method to learn the parameters under a unified framework. Generally speaking, these tensor methods are all based on lower-order moments of observed variables rather than the entire likelihood function. Notably, such tensor decompositions based on the lower-order moments are convex optimization problems, while maximizing the log-likelihood with latent variables is highly non-concave with potentially many local optima. As a result, an advantage of using moment-based tensor decomposition algorithms for learning latent variable models is the provable guarantee of converging to the global optimum of the objective function; see [Anandkumar et al. \(2014\)](#) for more details.

Besides the computational challenge, the second question of large-scale latent class analysis is how to ensure the estimators in the large- N and large- J regime are theoretically valid and meaningful. Traditionally, the subjects' latent class indicators in an LCM are often treated as random variables and marginalized out to obtain the marginal likelihood; we call the resulting model a random-effect LCM. On the other hand, an alternative approach is to treat the subjects' latent class indicators as fixed unknown parameters and directly incorporate them into the likelihood; we call the resulting model a fixed-effect LCM. In the classical scenario with sample size N going to infinity and the number of items J held fixed, the fixed-effect LCMs are known to be inconsistent for estimating the subject-level latent class indicators (e.g., see [Neyman and Scott, 1948](#)). However, for data featuring large N and large J , with an increasing amount of information collected per subject, an interesting theoretical question is whether we can obtain consistency in clustering the subjects

into their corresponding true latent class in fixed-effect LCMs?

In this paper, in the regime where both N and J go to infinity, we propose an efficient computational pipeline and develop the theory of clustering consistency for LCMs with binary responses. On the computational side, we propose an efficient two-step estimation pipeline integrating the moment-based tensor decomposition method and the EM algorithm. In the first step, we apply the tensor power method for LCMs to quickly and reliably find roughly accurate parameter estimates. In the second step, we use the tensor estimates as initialization for the EM algorithm to refine the parameter estimation. It is known that the method of moments can be viewed as good complementary to the maximum likelihood approach (Chaganty and Liang, 2013; Zhang et al., 2014; Balakrishnan et al., 2017). With good initialization, EM algorithms typically converge in very few iterations. Therefore, such an estimation pipeline combines the advantages of both the tensor decomposition algorithm and the EM algorithm for latent class analysis. Our extensive simulation studies empirically show that such an estimation pipeline enjoys both computational efficiency and estimation accuracy. Further, on the theoretical side, we prove the clustering consistency of the joint maximum likelihood estimator (joint MLE) for fixed-effect LCMs. That is, we prove that the joint MLE is consistent in estimating the subjects' latent class memberships under certain mild assumptions when N and J both go to infinity. We also derive a bound on the rate of convergence of the joint MLE's clustering performance.

The rest of this paper is organized as follows. The setups of random-effect and fixed-effect LCMs are introduced in Section 2. The proposed estimation procedures of large-scale LCM are presented in Section 3. Some preliminaries about tensor are also provided in Section 3 to make this section self-contained. Section 4 presents our theoretical results on clustering consistency of joint MLE. Section 5 presents simulation studies that evaluate the proposed estimation procedures and assess the empirical behavior of clustering consistency. A real data example is shown in Section 6, and we conclude this paper with some discussion in Section 7. The proof of the clustering consistency and additional simulation results are presented in Supplementary Material.

2 Latent Class Models with Binary Responses

In this section we introduce two perspectives of LCM. In random-effect LCMs, the latent class indicators are random variables; while in fixed-effect LCM, the latent class indicators are fixed and treated as unknown parameters. These two models share common assumptions on how the observed variables depend on the latent ones.

2.1 Latent Variables as Random Effects

We first introduce random-effect LCM. Consider a binary-outcome latent class model with J items and L classes. There are two types of individual-specific variables in the model, that is a binary response vector $R \in \{0, 1\}^J$ and a latent variable $z \in [L]$. Here $[L] = \{1, 2, \dots, L\}$ is the set of positive integers smaller than or equal to L . The response vector $R_i = (R_{i,1}, \dots, R_{i,J})$ contains the observed responses to the J items of i th subject. The j th component of R_i will be 1 if this subject gives a positive response to the j th item and will be 0 otherwise. For instance, in a test with J items, if a student answers the j th item correctly, then $R_{i,j}$, the j th component of R_i , will be 1. If the student fails to give a right answer then $R_{i,j} = 0$. The latent variable z_i is introduced to categorize different observations and explain the dependence among items.

The generative process for a response vector R_i of an observation is as follows: first the class of this observation z_i is drawn from a discrete distribution specified by the probability vector $\mathbf{p} = (p_1, p_2, \dots, p_L)$, where $p_k \geq 0$ and $\sum_{k=1}^L p_k = 1$. So we have

$$P(z_i = \ell) = p_\ell, \ell \in [L],$$

where p_ℓ is the proportion of subjects belonging to ℓ th class in the population. Then given the latent class $z_i = \ell$, the responses to J items are drawn conditionally independently from a Bernoulli distribution with parameter $\theta_{j,\ell}$ for each item j . That is

$$P(R_{i,j} = 1 | z_i = \ell) = \theta_{j,\ell}.$$

So $\theta_{j,\ell}$ measures the ability of subjects from ℓ th class to give a positive response on item j and is also known as item parameters. Like many other latent variables, local independence is assumed

here, implying the dependence of item responses is fully explained by the latent classes. We collect all the item parameters for the L classes in the matrix $\boldsymbol{\theta} = (\theta_{j,\ell}) \in [0, 1]^{J \times L}$ whose rows are indexed by the J items and columns indexed by the L classes. All the response vectors are collected in a $N \times J$ matrix \mathbf{R} , and the corresponding log-likelihood function under the random-effect LCM is

$$\ell(\mathbf{R}; \mathbf{p}, \boldsymbol{\theta}) = \log \left\{ \prod_{i=1}^N \left[\sum_{\ell=1}^L p_{\ell} \prod_{j=1}^J \theta_{j,\ell}^{R_{i,j}} (1 - \theta_{j,\ell})^{1-R_{i,j}} \right] \right\},$$

with $(\mathbf{p}, \boldsymbol{\theta})$ the parameters to be estimated.

2.2 Latent Variables as Fixed Effects

Another way to model latent classes is to view latent class assignment as fixed unknown parameters. For a fixed-effect LCM, denote the i th subject's latent class membership by a vector of binary entries $Z_{i,\cdot} = (Z_{i,1}, \dots, Z_{i,L})$, with $Z_{i,\ell} = 1$ if subject i belongs to the latent class ℓ . We also introduce another notation for the latent class membership $z_i \in \{1, 2, \dots, L\}$ and $z_i = \ell$ corresponds to $Z_{i,\ell} = 1$. Given a sample of size N , collect all the $Z_{1,\cdot}, \dots, Z_{N,\cdot}$ in a $N \times L$ matrix \mathbf{Z} , then each row of \mathbf{Z} contains only one entry of "1" and the remaining entries are zeros. We will use the two equivalent notations \mathbf{Z} and $\mathbf{z} = \{z_1, \dots, z_N\}$ interchangeably. The components of response vector R_i are independent Bernoulli variables with parameters specified by $\boldsymbol{\theta}$. So we have $P(R_{i,j} = 1) = \theta_{j,z_i}$. The log-likelihood for $(\mathbf{Z}, \boldsymbol{\theta})$ takes the following form

$$\begin{aligned} \ell(\mathbf{R}; \mathbf{Z}, \boldsymbol{\theta}) &= \log \left\{ \prod_{i=1}^N \prod_{\ell=1}^L \left[\prod_{j=1}^J (\theta_{j,\ell})^{R_{i,j}} (1 - \theta_{j,\ell})^{1-R_{i,j}} \right]^{Z_{i,\ell}} \right\} \\ &= \sum_i \sum_j \left\{ R_{i,j} \left[\sum_{\ell=1}^L Z_{i,\ell} \log(\theta_{j,\ell}) \right] + (1 - R_{i,j}) \left[\sum_{\ell=1}^L Z_{i,\ell} \log(1 - \theta_{j,\ell}) \right] \right\} \\ &= \sum_i \sum_j \left\{ R_{i,j} \log(\theta_{j,z_i}) + (1 - R_{i,j}) \log(1 - \theta_{j,z_i}) \right\}. \end{aligned} \tag{1}$$

The parameters to estimate are $(\mathbf{Z}, \boldsymbol{\theta})$. The above display is also called the complete data likelihood in the literature.

In fixed-effect LCM, if we imagine that \mathbf{z} is sampled from a discrete distribution which is separated from the sampling process of \mathbf{R} , the data generating process of fixed-effect LCM and

random-effect LCM coincides. So the estimation procedures developed in the following sections for random-effect LCM also apply to fixed-effect LCM.

3 Estimation Procedures

The EM algorithm is a popular method to maximize likelihood and estimate parameters in LCM by iterating between E-step and M-step. In E-step the probability of each subject belonging to each class is updated by current estimates of item parameters, and in M-step item parameters are updated given the probabilities of each subject’s latent class membership. However, the likelihood function under LCM is nonconcave due to the mixture model formulation. Hence, EM algorithm may suffer from convergence to local optima and slow convergence rate under poor initializations. Good initial values are critical to the success of the EM algorithm. In this section we introduce tensor method in [Anandkumar et al. \(2014\)](#) to find good initializations and hence improve the performance of EM algorithm. We will follow the discussions of [Anandkumar et al. \(2014\)](#) and be succinct and self-contained.

3.1 Preliminaries about Tensor

First we introduce some notations borrowed from [Anandkumar et al. \(2014\)](#). A real p -th order tensor $T \in \otimes_{i=1}^p \mathbb{R}^{n_i}$ is a p -way array of real numbers where $[T]_{i_1, \dots, i_p}$ is the (i_1, \dots, i_p) -th entry in the array. We will mostly consider the case where $n_i = n$ for all $i \in [p]$. Vectors and matrices are special cases of tensors where $p = 1$ and $p = 2$, respectively. Another view of tensor is that it is a multilinear map from a set of matrices $\{V_i \in \mathbb{R}^{n \times m_i} : i \in [p]\}$ to a p -th order tensor $T(V_1, \dots, V_p) \in \mathbb{R}^{m_1 \times \dots \times m_p}$ defined as

$$[T(V_1, \dots, V_p)]_{i_1, \dots, i_p} := \sum_{j_1, j_2, \dots, j_p} [T]_{j_1, j_2, \dots, j_p} [V_1]_{j_1, i_1} \dots [V_p]_{j_p, i_p}. \quad (2)$$

In this paper we will mainly consider three-way tensor and third-order case of this multilinear map. For a third-order tensor $T \in \otimes^3 \mathbb{R}^d$ and a vector $u \in \mathbb{R}^d$, we will make use of the following vector-valued map in the iteration of tensor power methods

$$T(I, u, u) = \sum_{i=1}^d \sum_{1 \leq j, l \leq d} [T]_{i, j, l} (e_j^T u) (e_l^T u) e_i \quad (3)$$

where e_1, \dots, e_d are the canonical basis vectors of \mathbb{R}^d ; that is, each e_k is a d -dimensional vector with only the k th entry being one and the other entries being zero. And we will also use the following map in the iteration

$$T(u, u, u) = \sum_{i,j,k} [T]_{i,j,k} (e_i^T u) (e_j^T u) (e_k^T u). \quad (4)$$

These maps are all special cases of (2).

Most tensors we consider in this paper are symmetric tensors, which means that an element of a tensor is invariant to permutations of its coordinates. If $T \in \otimes^p \mathbb{R}^d$ is a symmetric tensor, then we have $[T]_{i_1, \dots, i_p} = [T]_{i_{\pi(1)}, \dots, i_{\pi(p)}}$ for all permutations π on $[p]$. This concept is a generalization of symmetric matrices.

A simple case of a tensor is called rank-one tensor. A rank-one tensor $T \in \otimes^p \mathbb{R}^d$ can be expressed as tensor product of p vectors: $T = v_1 \otimes v_2 \otimes \dots \otimes v_p$ for some vectors $v_1, \dots, v_p \in \mathbb{R}^d$, where $[T]_{i_1, \dots, i_p} = \prod_{k=1}^p [v_k]_{i_k}$ and $[v_k]_{i_k}$ is the i_k th component of v_k . When $v_k = v$ for all k , we can get a symmetric tensor. More detailed discussion and introductions about tensor can be found in [Kolda and Bader \(2009\)](#).

3.2 Tensor Structure in Random-Effect LCM

[Anandkumar et al. \(2014\)](#) showed that for some latent variable models, their low-order moments can be expressed as a sum of rank-one tensors. Once this structure of cross moments is obtained for a particular model, one can apply the orthogonal tensor decomposition to learn the parameters of the model. For random-effect LCM, we show that there is also useful tensor structure in low-order moments by examining Theorem 3.6 in [Anandkumar et al. \(2014\)](#), which studies the multi-view models.

Recall that we use R to generally denote a response vector of length J . We consider R on a population level and divide the items into three disjoint parts (so we assume $J \geq 3$) R^1, R^2, R^3 with each $R^t \in \mathbb{R}^{J^t}$ and $J_1 + J_2 + J_3 = J$. The item parameters of R^t are denoted by $\theta_t \in \mathbb{R}^{J^t \times L}$, which is a sub-matrix of θ , with rows corresponding to rows in R^t . We need the following assumption to derive the tensor structure.

Condition 1. *Each θ_t has full column rank for $t = 1, 2, 3$.*

Note that the partition of items can be arbitrary as long as the item parameters for each part satisfy Condition 1. So we can try different partitions to estimate the parameters and take average to obtain the final estimates.

We denote the i th column of $\boldsymbol{\theta}_t$ to be $\boldsymbol{\theta}_{t,i}$. The following theorem restates Theorem 3.6 in [Anandkumar et al. \(2014\)](#) in our setting and characterizes the tensor structure in random-effect LCM.

Theorem 1. *Assume that Condition 1 holds and $p_1, \dots, p_L > 0$. Define*

$$\begin{aligned}
R^{2'} &:= \mathbb{E}[R^1 \otimes R^3] \mathbb{E}[R^2 \otimes R^3]^+ R^2 \\
R^{3'} &:= \mathbb{E}[R^1 \otimes R^2] \mathbb{E}[R^3 \otimes R^2]^+ R^3 \\
M_2 &:= \mathbb{E}[R^1 \otimes R^{2'}] \\
M_3 &:= \mathbb{E}[R^1 \otimes R^{2'} \otimes R^{3'}]
\end{aligned} \tag{5}$$

where A^+ denotes the Moore-Penrose pseudoinverse of matrix A . Then we have

$$\begin{aligned}
M_2 &= \sum_{i=1}^L p_i \boldsymbol{\theta}_{1,i} \otimes \boldsymbol{\theta}_{1,i}, \\
M_3 &= \sum_{i=1}^L p_i \boldsymbol{\theta}_{1,i} \otimes \boldsymbol{\theta}_{1,i} \otimes \boldsymbol{\theta}_{1,i}.
\end{aligned} \tag{6}$$

Proof. First we compute the cross moment. For $t \neq t'$, R^t and $R^{t'}$ are conditionally independent, we have

$$\mathbb{E}[R^t \otimes R^{t'}] = \sum_{i=1}^L p_i \mathbb{E}[R^t \otimes R^{t'} | z = i] = \sum_{i=1}^L p_i \mathbb{E}[R^t | z = i] \otimes \mathbb{E}[R^{t'} | z = i] = \sum_{i=1}^L p_i \boldsymbol{\theta}_{t,i} \otimes \boldsymbol{\theta}_{t',i}.$$

If we denote $D = \text{diag}\{p_1, \dots, p_L\}$, then we have $\mathbb{E}[R^t \otimes R^{t'}] = \boldsymbol{\theta}_t D \boldsymbol{\theta}_{t'}^\top$. Then we calculate the conditional mean

$$\mathbb{E}[R^{2'} | z = i] = \mathbb{E}[R^1 \otimes R^3] \mathbb{E}[R^2 \otimes R^3]^+ \mathbb{E}[R^2 | z = i].$$

According to the model setting $\mathbb{E}[R^2 | z = i] = \boldsymbol{\theta}_2 e_i$, then we have

$$\mathbb{E}[R^{2'} | z = i] = \boldsymbol{\theta}_1 D \boldsymbol{\theta}_3^\top (\boldsymbol{\theta}_2 D \boldsymbol{\theta}_3^\top)^+ \boldsymbol{\theta}_2 e_i = \boldsymbol{\theta}_1 D (\boldsymbol{\theta}_3^+ \boldsymbol{\theta}_3)^\top D^{-1} \boldsymbol{\theta}_2^+ \boldsymbol{\theta}_2 e_i.$$

By condition 1, $\boldsymbol{\theta}_t^+ \boldsymbol{\theta}_t = I_L$ for all t , thus $\mathbb{E}[R^{2'} | z = i] = \boldsymbol{\theta}_{1,i}$. Similarly, $\mathbb{E}[R^{3'} | z = i] = \boldsymbol{\theta}_{1,i}$. So we have

$$M_2 = \sum_{i=1}^L p_i \mathbb{E}[R^1 \otimes R^{2'} | z = i] = \sum_{i=1}^L p_i \mathbb{E}[R^1 | z = i] \otimes \mathbb{E}[R^{2'} | z = i] = \sum_{i=1}^L p_i \boldsymbol{\theta}_{1,i} \otimes \boldsymbol{\theta}_{1,i}.$$

Similarly one can get the decomposition for M_3 in (6). \square

In applications we only have finite samples and the moments in Theorem 1 should be approximated by empirical moments. In particular, once we have samples $R_1, \dots, R_N \in \mathbb{R}^J$, we partition each sample and obtain $R_i^t \in \mathbb{R}^{J^t}$ corresponding to the partition on population level. Then the transformed response and estimated moments can be computed by

$$\begin{aligned}
\widehat{\mathbb{E}}[R^t \otimes R^{t'}] &:= \frac{1}{N} \sum_{j=1}^N R_j^t \otimes R_j^{t'} \\
\widehat{R}_i^{2'} &:= \widehat{\mathbb{E}}[R^1 \otimes R^3] \left(\widehat{\mathbb{E}}[R^2 \otimes R^3] \right)^+ R_i^2 \\
\widehat{R}_i^{3'} &:= \widehat{\mathbb{E}}[R^1 \otimes R^2] \left(\widehat{\mathbb{E}}[R^3 \otimes R^2] \right)^+ R_i^3 \\
\widehat{M}_2 &:= \frac{1}{N} \sum_{j=1}^N R_j^1 \otimes \widehat{R}_j^{2'}, \\
\widehat{M}_3 &:= \frac{1}{N} \sum_{j=1}^N R_j^1 \otimes \widehat{R}_j^{2'} \otimes \widehat{R}_j^{3'}.
\end{aligned} \tag{7}$$

Due to the randomness of sample, it is possible that $r =: \text{rank}(\widehat{\mathbb{E}}[R^2 \otimes R^3]) > L$ and $(\widehat{\mathbb{E}}[R^2 \otimes R^3])$ has $(r - L)$ extra non-zero singular values. These singular values will be small since they equal to 0 in $(\widehat{\mathbb{E}}[R^2 \otimes R^3])$'s population counterpart $\mathbb{E}[R^2 \otimes R^3]$. In this case we should discard these extra singular values and only use first L singular values when calculating $(\widehat{\mathbb{E}}[R^2 \otimes R^3])^+$, otherwise one has to compute the inverse of these small singular values which will incur large error.

After learning θ_1 from data by the tensor power method to be introduced in Section 3.3, we can obtain θ_2 and θ_3 by setting $\theta_2 = \mathbb{E}[R^2 \otimes R^3] \mathbb{E}[R^1 \otimes R^3]^+ \theta_1$ and $\theta_3 = \mathbb{E}[R^3 \otimes R^2] \mathbb{E}[R^1 \otimes R^2]^+ \theta_1$. This can be derived in a same way as Theorem 1. So the main problem is to estimate θ_1 from moments M_2 and M_3 .

Although this structure only holds for random-effect LCMs, as we mentioned above, in fixed-effect LCMs we can view z_1, \dots, z_N as random. For instance, they are sampled from some discrete distributions on $[L]$ independently from \mathbf{R} . Then the data generation process of random-effect and fixed-effect LCMs are the same and the estimation procedures for random-effect LCMs also apply to fixed-effect LCMs.

3.3 Tensor Method to Learn the Parameters

In this section we briefly describe the procedures in [Anandkumar et al. \(2014\)](#) to recover the parameters in (6). That is, given

$$\begin{aligned} M_2 &= \sum_{i=1}^L w_i \mu_i \otimes \mu_i, \\ M_3 &= \sum_{i=1}^L w_i \mu_i \otimes \mu_i \otimes \mu_i \end{aligned} \tag{8}$$

where $\mu_i \in \mathbb{R}^d$, we want to obtain the elements of decomposition (w_i, μ_i) 's from M_2 and M_3 . Condition 1 now becomes $\{\mu_1, \dots, \mu_L\}$ are linearly independent. First we introduce the orthogonal decomposition of a tensor. Then we see how we can use tensor power method to recover the orthogonal decomposition of a tensor and estimate the parameters.

3.3.1 Orthogonal Decomposition

Since the moments structures in (8) are about at most a third-order tensor, we only consider the case $p = 3$ (third-order tensor).

A symmetric tensor $T \in \otimes^3 \mathbb{R}^d$ has an orthogonal decomposition if there exists a collection of orthonormal unit vectors $\{v_1, \dots, v_L\}$ and positive scalars $\lambda_i > 0$ such that

$$T = \sum_{i=1}^L \lambda_i v_i \otimes v_i \otimes v_i. \tag{9}$$

Without loss of generality we assume $\lambda_i > 0$ because for third-order tensor we have $-\lambda_i v_i^{\otimes 3} = \lambda_i (-v_i)^{\otimes 3}$. This is a generalization of spectral decomposition for a symmetric matrix. We can also generalize the concept of eigenvalue and eigenvectors.

Recall the definition of the multilinear map induced by a tensor in (2). A unit vector $u \in \mathbb{R}^d$ is an eigenvector of T with corresponding eigenvalue $\lambda \in \mathbb{R}$ if $T(I, u, u) = \lambda u$. For an orthogonally decomposable tensor $T = \sum_{i=1}^L \lambda_i v_i \otimes v_i \otimes v_i$, one can check operation (3) is

$$T(I, u, u) = \sum_{i=1}^L \lambda_i (u^T v_i)^2 v_i$$

and operation (4) reduces to

$$T(u, u, u) = \sum_{i=1}^L \lambda_i (u^T v_i)^3.$$

By the orthogonality of v_i 's, $T(I, v_i, v_i) = \lambda_i v_i$ and $T(v_i, v_i, v_i) = \lambda_i$ for all $i \in [L]$. Thus (λ_i, v_i) is an eigenpair of T .

The eigenpairs of a tensor are more complicated than those of a matrix and there are some subtle points; see [Anandkumar et al. \(2014\)](#) for more discussion. Fortunately, Theorem 4.1 and 4.2 in [Anandkumar et al. \(2014\)](#) guarantee the uniqueness and identifiability of orthogonal decomposition in (9).

3.3.2 Whitening Process

Comparing the third-order moment structure M_3 in (8) with the orthogonal decomposition form (9), we find they have almost the same form except that the vectors μ_i 's in (8) may not necessarily be orthogonal to each other. So we need to whiten the tensor M_3 to \widetilde{M}_3 , which has an orthogonal decomposition. In the whitening process we will make use of M_2 in (8).

Let $W \in \mathbb{R}^{d \times L}$ satisfy $M_2(W, W) = W^T M_2 W = I_L$. We can take $W = UD^{-1/2}$, where D is the diagonal matrix containing all positive eigenvalues of M_2 and $U \in \mathbb{R}^{d \times L}$ is the matrix of corresponding orthogonal eigenvectors of M_2 . $D^{-1/2}$ is well-defined since we assume μ_i 's are linearly independent and thus M_2 is of rank L .

Define $\widetilde{\mu}_i := \sqrt{\omega_i} W^T \mu_i$ and observe that

$$M_2(W, W) = \sum_{i=1}^L W^T (\sqrt{\omega_i} \mu_i) (\sqrt{\omega_i} \mu_i)^T W = \sum_{i=1}^L \widetilde{\mu}_i \widetilde{\mu}_i^T = I_L.$$

So $\widetilde{\mu}_i$'s are orthonormal vectors.

Define

$$\widetilde{M}_3 := M_3(W, W, W) = \sum_{i=1}^L \omega_i (W^T \mu_i)^{\otimes 3} = \sum_{i=1}^L \frac{1}{\sqrt{\omega_i}} \widetilde{\mu}_i^{\otimes 3}.$$

Since $\widetilde{\mu}_i$'s are orthonormal vectors, this is the orthogonal decomposition of \widetilde{M}_3 . We can use tensor power method described in section 3.3.3 to obtain the eigenpairs $(\lambda_i, v_i) = (1/\sqrt{\omega_i}, \widetilde{\mu}_i)$. Then we can recover the parameters ω_i 's, μ_i 's as $(\omega_i, \mu_i) = (\frac{1}{\lambda_i^2}, \lambda_i (W^T)^+ \widetilde{\mu}_i)$, where $(W^T)^+$ is the Moore-Penrose pseudoinverse of W^T .

3.3.3 Tensor Power Method

Now we show how to recover the parameters (λ_i, v_i) 's in (9) from a tensor T . In analogy to matrix power method, here we use the tensor power method of De et al. (2000) to obtain the eigenpairs (λ_i, v_i) in (9). First suppose a third-order tensor has an exact orthogonal decomposition. Then we have the following result on the algorithmic convergence of tensor power method (Lemma 5.1 in Anandkumar et al. (2014)).

Theorem 2. *Let $T \in \otimes^3 \mathbb{R}^d$ have an orthogonal decomposition as given in (9). For a vector $\theta_0 \in \mathbb{R}^d$, suppose that the set of numbers $\{|\lambda_i v_i^\top \theta_0|, 1 \leq i \leq L\}$ has a unique largest value. For $t = 1, 2, \dots$, let*

$$\theta_t := \frac{T(I, \theta_{t-1}, \theta_{t-1})}{\|T(I, \theta_{t-1}, \theta_{t-1})\|}.$$

Then

$$\|v_1 - \theta_t\|^2 \leq (2\lambda_1^2 \sum_{i=2}^K \lambda_i^{-2}) \left| \frac{\lambda_2 v_2^\top \theta_0}{\lambda_1 v_1^\top \theta_0} \right|^{2^{t+1}}.$$

So repeated iteration starting from θ_0 converges to v_1 . To obtain all the eigenpairs, we use “deflation” after getting an eigenpair (λ_i, v_i) . That is, to obtain the j -th eigenpair, we subtract the previous $j - 1$ rank-one structures from T and then execute the power method on $T - \sum_{i=1}^{j-1} \lambda_i v_i \otimes v_i \otimes v_i$.

However, in practice we plug-in the empirical estimate of M_2 and M_3 in (6) and the estimate of whitened tensor \widetilde{M}_3 may not have an exact orthogonal decomposition. So we should consider the case where we only have an approximation \widehat{T} of T and need a more robust algorithm to use an orthogonal decomposition to approximate \widehat{T} . Following Anandkumar et al. (2014), we present the following Algorithm 1. Multiple starting points are used in Algorithm 1 to ensure approximate convergence at first stage. Intuitively, by restarting from different points we can start from a point from which the initial n iteration from it dominates the error $\widehat{T} - T$. Perturbation analysis (Theorem 5.1 in Anandkumar et al. (2014)) shows that we can find such a point with high probability with $K = \text{poly}(L)$ trials. In our simulation settings we find tensor estimator is good enough as initializations for EM algorithm with $K = 10$ trials on starting points.

In conclusion, the procedures to learn (ω_i, μ_i) from M_2 and M_3 in (8) are : (1) Use the information of M_2 to whiten M_3 and get \widetilde{M}_3 ; (2) Apply tensor power method to \widetilde{M}_3 and learn the orthogonal

Algorithm 1 Robust tensor power method

Input: symmetric tensor $\tilde{T} \in \mathbb{R}^{d \times d \times d}$, number of iterations K , n .

Output: estimates of one of eigenpairs; the deflated tensor

- 1: **for** $\tau = 1$ to K **do**
- 2: Draw $\theta_0^{(\tau)}$ uniformly from unit sphere in \mathbb{R}^d .
- 3: **for** $t = 1$ to n **do**
- 4: Compute power iteration and re-normalization

$$\theta_t^{(\tau)} = \frac{\tilde{T}(I, \theta_{t-1}^{(\tau)}, \theta_{t-1}^{(\tau)})}{\|\tilde{T}(I, \theta_{t-1}^{(\tau)}, \theta_{t-1}^{(\tau)})\|}$$

- 5: **end for**
 - 6: **end for**
 - 7: Let $\tau^* = \operatorname{argmax}_{\tau \in [K]} \{\tilde{T}(\theta_{t-1}^{(\tau)}, \theta_{t-1}^{(\tau)}, \theta_{t-1}^{(\tau)})\}$
 - 8: Do n power iteration updates further starting from $\theta_n^{(\tau^*)}$ to obtain $\hat{\theta}$, and set $\hat{\lambda} = \tilde{T}(\hat{\theta}, \hat{\theta}, \hat{\theta})$.
 - 9: **return** the estimated eigenpair $(\hat{\lambda}, \hat{\theta})$; the deflated tensor $T - \hat{\lambda} \hat{\theta} \otimes \hat{\theta} \otimes \hat{\theta}$.
-

decomposition of it; (3) Obtain the original parameters with an inverse transformation of whitening. In application we can plug-in the estimates of M_2 and M_3 and learn the parameters from samples.

In our random-effect LCM, we can apply this procedure to (6) and learn p_i 's and θ . When the sample size is large enough, this method alone can yield an estimator close to the true parameters. However if we do not have so many samples, estimates based on tensor are not so accurate since in tensor method we only take advantage of low-order moments and ignore other information of sampling distributions. So after obtaining the tensor estimates, we use them as initial values for EM algorithms to improve the accuracy. For fixed-effect LCM, we first learn p_i 's and θ from (6) as a initialization step and apply Classification-EM (CEM) algorithm proposed in [Celeux and Govaert \(1992\)](#) to obtain the final estimator. We call this two-step estimation procedure the *tensor-EM method*.

Empirically, we find that the accuracy of this method is comparable to estimates obtained with EM algorithm starting from true parameters, indicating that the tensor-EM method can give the MLE of latent class model when the model is correct. Moreover, it is more computationally

efficient than EM algorithm with several random initial values, especially in large-scale data. See our simulation study for more details.

3.4 Selecting the Number of Classes

In the discussion above we assume the number of classes L is known. Next we discuss the model selection of L . There exists a rich literature in selecting number of classes. [Nylund et al. \(2007\)](#) performed a Monte Carlo simulation study on several commonly used methods and found BIC proposed in [Schwarz \(1978\)](#) and likelihood ratio test based on bootstrap in [McLachlan and Peel \(2004\)](#) have a better performance. They recommend BIC and likelihood ratio test based on bootstrap to select the number of classes. Since we focus on large-scale datasets containing many items and samples, we follow the discussion of [Chen et al. \(2017\)](#) and apply generalized information criterion proposed in [Nishii \(1984\)](#) to selecting the number of classes.

Specifically, for a candidate set \mathcal{L} and any $L \in \mathcal{L}$, we apply the tensor-EM algorithm to learning the parameters and compute the generalized information criterion for random-effect and fixed-effect LCM as follows:

$$\text{GIC}_R(L) = -2 \ell(\mathbf{R}; \hat{\mathbf{p}}^L, \hat{\boldsymbol{\theta}}^L) + a_N \dim(\mathbf{p}, \boldsymbol{\theta}),$$

$$\text{GIC}_F(L) = -2 \ell(\mathbf{R}; \hat{\mathbf{Z}}^L, \hat{\boldsymbol{\theta}}^L) + a_N \dim(\mathbf{Z}, \boldsymbol{\theta})$$

where $\dim(\mathbf{p}, \boldsymbol{\theta})$ is the dimension of parameters to estimate and measures the model complexity. We have $\dim(\mathbf{p}, \boldsymbol{\theta}) = JL + L - 1$ in random-effect LCM and $\dim(\mathbf{Z}, \boldsymbol{\theta}) = JL + N$ in fixed-effect LCM. Sample size dependent quantity a_N measures the level of penalty on model complexity. Here we consider two choice of a_N .

- GIC_1 : $a_N = \log(N)$. This case corresponds to BIC and it enjoys some consistent results shown in [Nishii \(1984\)](#) when the model has low complexity (i.e. the dimension of parameters is fixed).
- GIC_2 : $a_N = \log[\log(N)]\log N$. This choice is considered in [Fan and Tang \(2013\)](#) in generalized linear model to address the case where the dimension of parameter space d increases at a polynomial order of N , that is, $d = O(N^c)$ for some $c > 0$. The large-scale latent class model

we consider tends to have many items and the dimension of parameters $\dim(\boldsymbol{p}, \boldsymbol{\theta}) = J \times L + L - 1$ can be large and should not be treated as fixed. For instance, in the simulation study a random-effect LCM we consider has ten classes and one hundred items. This model has dimension $d = 1009$ while the sample size is $N = 1000$. So it is appropriate to adopt this choice in this setting. See [Fan and Tang \(2013\)](#) for discussion about theoretical results of this choice of a_N .

After calculating the GIC for different models, we select the number of classes to minimize $\text{GIC}(L)$:

$$L^* = \arg \min_{L \in \mathcal{L}} \text{GIC}(L).$$

Although our simulation results show that the tensor-EM method gives the MLE of the model when the number of classes L is correctly selected, it may converge to some local optima when L is incorrect. It is also likely that the tensor method yields inaccurate results when L is misspecified as \tilde{L} . For instance, some item parameters may be negative or over one, which happens when the sample size is small. In this case, we propose to revise the tensor estimates as follows: we set the negative components to be a small positive number (e.g. 0.001) and those over one to be a number close to 1 (e.g. 0.999). Such a procedure will help us select the number of classes because we know as long as the true number of classes is specified, the tensor-EM method can yield an ideal estimate (MLE) with a small GIC value. On the other hand, a poor estimate based on a misspecified model will give a larger GIC value, indicating misfit of the model. Hence, GIC values computed by tensor-EM method can provide useful information to select the number of classes. According to our simulation study, the proposed method can select the right model most of the time.

After proposing the computational methods to select number of classes and to find the MLE, we next examine the theoretical properties of MLE in the large- N and large- J scenario. For random-effect LCM with fixed number of items J , the MLE is known to be consistent. However, the joint MLE for fixed-effect LCM may not be consistent ([Neyman and Scott, 1948](#)) when J is fixed. Intuitively, one cannot hope to recover each subject's latent class membership accurately with only a finite number of items observed for each subject. So in the next section, we will consider the consistency of joint MLE when J also goes to infinity in fixed-effect LCMs.

4 Clustering Consistency of the Joint MLE

In this section we consider large-scale fixed-effect LCMs and characterize the behavior of latent class assignment estimator $\widehat{\mathbf{Z}}$ under suitable conditions, where $(\widehat{\boldsymbol{\theta}}, \widehat{\mathbf{Z}})$ is the joint maximum likelihood estimator (MLE). We use a similar proof technique as in [Gu and Xu \(2020\)](#) to establish the clustering consistency of the joint MLE for fixed-effect LCMs.

First we need to define some notations. Denote the true parameters by $(\boldsymbol{\theta}^0, \mathbf{Z}^0)$. Define

$$P_{i,j} = \mathbb{P}(R_{i,j} = 1) = \theta_{j,z_i^0}^0,$$

$$M = \frac{1}{NJ} \sum_{i=1}^N \sum_{j=1}^J \mathbb{P}(R_{i,j} = 1).$$

The $M \in [0, 1]$ above measures the average positive response rate over all subjects and items. Denote the expectation of log-likelihood $\ell(\mathbf{R}; \mathbf{Z}, \boldsymbol{\theta})$ in (1) by

$$\bar{\ell}(\mathbf{Z}, \boldsymbol{\theta}) = \mathbb{E}[\ell(\mathbf{R}; \mathbf{Z}, \boldsymbol{\theta})] = \sum_{i=1}^N \sum_{j=1}^J \left\{ P_{i,j} \log(\theta_{j,z_i}) + (1 - P_{i,j}) \log(1 - \theta_{j,z_i}) \right\},$$

where the expectation is taken with respect to the distribution of \mathbf{R} .

Given arbitrary \mathbf{Z} , denote

$$\ell(\mathbf{R}; \mathbf{Z}) = \sup_{\boldsymbol{\theta}} \ell(\mathbf{R}; \mathbf{Z}, \boldsymbol{\theta}) = \ell(\mathbf{R}; \mathbf{Z}, \widehat{\boldsymbol{\theta}}^{(\mathbf{Z})}),$$

$$\bar{\ell}(\mathbf{Z}) = \sup_{\boldsymbol{\theta}} \bar{\ell}(\mathbf{Z}, \boldsymbol{\theta}) = \bar{\ell}(\mathbf{Z}, \bar{\boldsymbol{\theta}}^{(\mathbf{Z})}),$$

where $\widehat{\boldsymbol{\theta}}^{(\mathbf{Z})} = \arg \max_{\boldsymbol{\theta}} \ell(\mathbf{R}; \mathbf{Z}, \boldsymbol{\theta})$ and $\bar{\boldsymbol{\theta}}^{(\mathbf{Z})} = \arg \max_{\boldsymbol{\theta}} \bar{\ell}(\mathbf{Z}, \boldsymbol{\theta})$. Then under any realization of \mathbf{Z} , the following holds for any latent class $a \in [L]$,

$$\widehat{\theta}_{j,a}^{(z)} = \frac{\sum_i Z_{i,a} R_{i,j}}{\sum_i Z_{i,a}}, \quad \bar{\theta}_{j,a}^{(z)} = \frac{\sum_i Z_{i,a} P_{i,j}}{\sum_i Z_{i,a}}. \quad (10)$$

We consider the joint maximum likelihood estimator $(\widehat{\boldsymbol{\theta}}, \widehat{\mathbf{Z}})$ subject to fitting a L -class fixed-effect LCM with true parameters $(\boldsymbol{\theta}^0, \mathbf{Z}^0)$,

$$(\widehat{\boldsymbol{\theta}}, \widehat{\mathbf{Z}}) = \arg \max_{(\boldsymbol{\theta}, \mathbf{Z})} \ell(\mathbf{R}; \mathbf{Z}, \boldsymbol{\theta}).$$

Note that $\widehat{\mathbf{Z}} = \arg \max_{\mathbf{Z}} \ell(\mathbf{R}; \mathbf{Z}, \widehat{\boldsymbol{\theta}}^{(\mathbf{Z})}) = \arg \max_{\mathbf{Z}} \ell(\mathbf{R}; \mathbf{Z})$, where $\widehat{\boldsymbol{\theta}}^{(\mathbf{Z})}$ maximizes the profile likelihood $\ell(\mathbf{R}; \mathbf{Z}, \boldsymbol{\theta})$ given a particular realization \mathbf{Z} . In [Section 3](#) we will discuss procedures to compute the joint MLE efficiently.

We impose the following assumptions on the true parameters.

Assumption 1. *There exists a constant $d > 0$ such that*

$$\frac{1}{J^d} \leq \min_{\substack{1 \leq j \leq J, \\ 1 \leq a \leq L}} \theta_{j,a}^0 \leq \max_{\substack{1 \leq j \leq J, \\ 1 \leq a \leq L}} \theta_{j,a}^0 \leq 1 - \frac{1}{J^d}. \quad (11)$$

Assumption 2. *There exists a positive sequence $\{\beta_J\}$ such that*

$$\frac{1}{J} \min_{1 \leq a \neq b \leq L} \|\boldsymbol{\theta}^0_{:,a} - \boldsymbol{\theta}^0_{:,b}\|^2 \geq \beta_J, \quad (12)$$

where $\|\cdot\|$ denotes the ℓ_2 norm.

Assumption 1 guarantees that the components of $\boldsymbol{\theta}$ are bounded away from 0 and 1 but allowed to become very close to 0 or 1 as J becomes larger. It is a quite mild technical assumption. Assumption 2 is an identification condition for latent classes and guarantees that the item parameters of different class are different enough. Note that we allow different classes to have same probability to answer a single item correctly (i.e. $\theta_{j,a} = \theta_{j,b}$ for some $a \neq b$). But their average performance on the J items should be different.

In fitting the latent class model, we are interested in controlling the number of incorrect latent class assignments. Formally, after obtaining some estimator $\widehat{\mathbf{z}}$, let $\widehat{C}_1, \dots, \widehat{C}_L$ be clusters from our estimator $\widehat{\mathbf{z}}$ such that subjects sharing same estimated membership are in one cluster. Let $m_l = \arg \max_{a \in [L]} \sum_{i \in \widehat{C}_l} Z_{i,a}^0$ be the majority of true class membership among subjects in \widehat{C}_l . Since the latent classes are identified up to permutations of class index, m_l should be viewed as the class index of \widehat{C}_l corresponding to true class assignments \mathbf{z}^0 . The number of incorrect class assignments under estimated latent class assignments $N_e(\widehat{\mathbf{z}})$ is defined as:

$$N_e(\widehat{\mathbf{z}}) = N - \sum_{l=1}^L \left| \{i \in \widehat{C}_l : Z_{i,m_l}^0 = 1\} \right| \quad (13)$$

So every subject $i \in \{1, \dots, N\}$ whose true class under \mathbf{z}^0 is not in the majority within its estimated class under $\widehat{\mathbf{z}}$ is counted. For instance, if we have eight subjects from two classes and we end up with estimated clusters $\widehat{C}_1 = \{1, 1, 1, 1, 2\}$ and $\widehat{C}_2 = \{1, 2, 2\}$, where “1” and “2” represents the true class index for each subject. Then $m_1 = 1$, $m_2 = 2$ and number of errors $N_e(\widehat{\mathbf{z}}) = 2$.

We have the following main theorem on the clustering consistency of joint MLE for fixed-effect LCM, which characterizes the asymptotic behavior of error rate $N(\widehat{\mathbf{z}})/N$.

Theorem 3. Under assumptions 1 and 2, assume $N, J \rightarrow \infty$, L is fixed and

$$\frac{J}{MN^{2(1-\xi)}} \rightarrow 0 \quad \text{for some small } \xi > 0, MJ \rightarrow \infty,$$

for the joint maximum likelihood estimator $\hat{\mathbf{z}}$, we have

$$\frac{N_e(\hat{\mathbf{z}})}{N} = o_P \left(\frac{(\log J)^{1+\eta} \cdot \sqrt{M}}{\sqrt{J}\beta_J} \right) \quad (14)$$

for any $\eta > 0$.

Assigning each subject to latent class resembles the process of clustering and hence we name our results as “clustering consistency”. In particular if $M = \frac{1}{NJ} \sum_{i=1}^N \sum_{j=1}^J \mathbb{P}(R_{i,j} = 1)$ is of the constant order (denoted by $M = \Theta(1)$), the only scaling condition would become $J = o(N^{2(1-\xi)})$ for some small $\xi > 0$ and this is very mild. The rate depends on β_J specified in (12). If the item parameters between different classes differ by a constant then we have $\beta_J = \Theta(1)$ and the final error rate $N_e(\hat{\mathbf{z}})/N = o_P \left((\log J)^{1+\eta}/\sqrt{J} \right)$ and decays towards zero as N, J increases.

5 Simulation Study

5.1 Performance of tensor-EM method

In this section we perform simulation studies to assess the performance of the tensor-EM method. We consider 24 different settings: $\{N = 1000, 10000, 20000\} \otimes \{J = 100, 200\} \otimes \{L = 5, 10\} \otimes \{\text{item parameters} \in \{0.1, 0.2, 0.8, 0.9\} \text{ or } \{0.2, 0.4, 0.6, 0.8\}\}$. By item parameters $\in \{0.1, 0.2, 0.8, 0.9\}$ we mean we generate the true θ 's elements $\theta_{j,a}$ independently and uniformly from $\{0.1, 0.2, 0.8, 0.9\}$. Note that the considered large-scale LCM with many items, the generic identifiability conditions stated in Corollary 5 in Allman et al. (2009) is guaranteed.

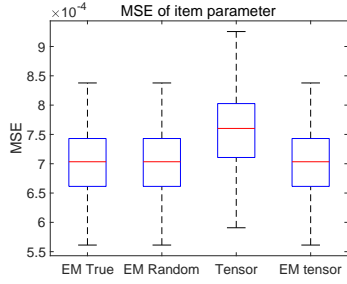
We compare the performance of the proposed tensor-EM method with three other methods:

- (1) EM-true, which is the EM algorithm starting from the true parameters as initial values;
- (2) EM-random, where we randomly generate the initial values for the EM algorithm and repeat five times, and then we select the estimators corresponding to maximum log-likelihood;

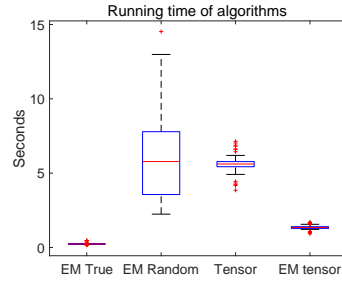
(3) the tensor power method alone. In this third competitor, we permute the items randomly and obtain a tensor estimate for each permutation. Let π be a permutation of $[J]$ and R^π be subject response vector corresponding to permutation π (i.e. $[R^\pi]_i = R_{\pi(i)}$). We obtain tensor estimates $\hat{\boldsymbol{\theta}}^\pi$ from cross moments of R^π and set the tensor estimates of original item parameters as $\hat{\theta}_{j,a} = \hat{\theta}_{\pi^{-1}(j),a}^\pi$. We then repeat this procedure five times and finally take average of them. This repetition can reduce the MSE of item parameters a little but will remain the same magnitude.

We emphasize that in the proposed tensor-EM method, we do not repeat the tensor power method or take any average. Empirically, just one implementation of the tensor power method gives good initial values for the EM algorithm.

The running time and MSE are reported, where $\text{MSE} = \sum_{j=1}^J \sum_{l=1}^L (\theta_{j,l} - \hat{\theta}_{j,l})^2 / (JL)$. In some settings, the EM-random estimates have too large MSEs, so we also present the plots excluding the EM-random estimates to better visualize the MSEs of the other three methods. The results are based on 100 replications in each simulation setting. For the random-effect LCM, the population proportion vector \boldsymbol{p} and item parameters $\boldsymbol{\theta}$ are first generated and the process of generating samples and estimation is repeated. The proportion vector \boldsymbol{p} is generated randomly to guarantee each class has enough samples (in settings with five classes we have $p_a \geq 0.1$ and in settings with ten classes we have $p_a \geq 0.08$ for all a). For the fixed-effect LCM, the latent class membership \mathbf{Z} and $\boldsymbol{\theta}$ are generated and the process of sampling and estimation is repeated (so unlike in random-effect LCM, \mathbf{Z} is the same for each replication). Due to the space limitation, we present here three representative figures for each type of LCM (i.e., random-effect LCM and fixed-effect LCM) in Figures 1–6, and provide the rest simulation results in Supplementary Material.

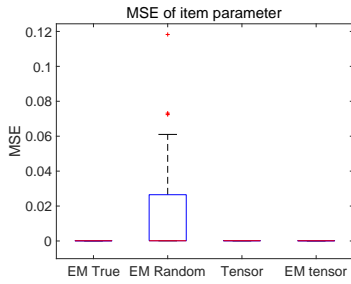


(a) MSE of item parameters

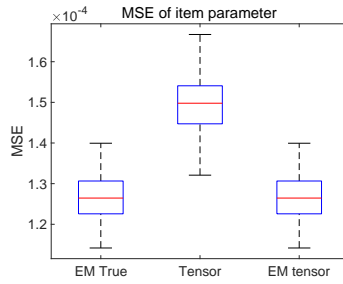


(b) Running time of the algorithms

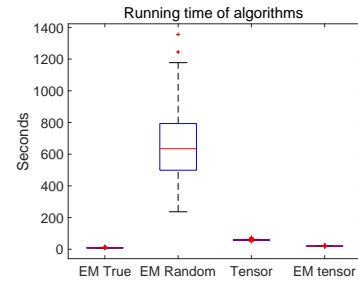
Figure 1: Random-effect LCM, $N = 1000, J = 100, L = 5, \theta_{j,a} \in \{0.1, 0.2, 0.8, 0.9\}$



(a) MSE of item parameters

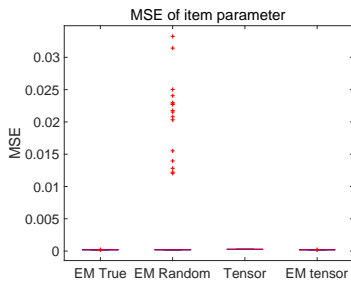


(b) MSE without EM-random

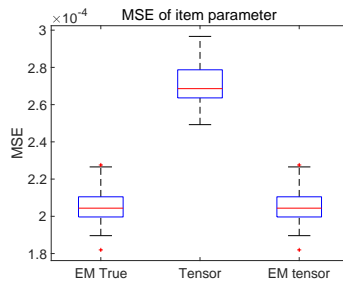


(c) Running time of the algorithms

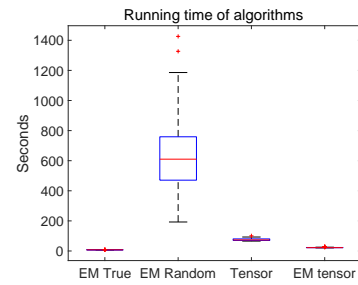
Figure 2: Random-effect LCM, $N = 10000, J = 100, L = 10, \theta_{j,a} \in \{0.1, 0.2, 0.8, 0.9\}$



(a) MSE of item parameters

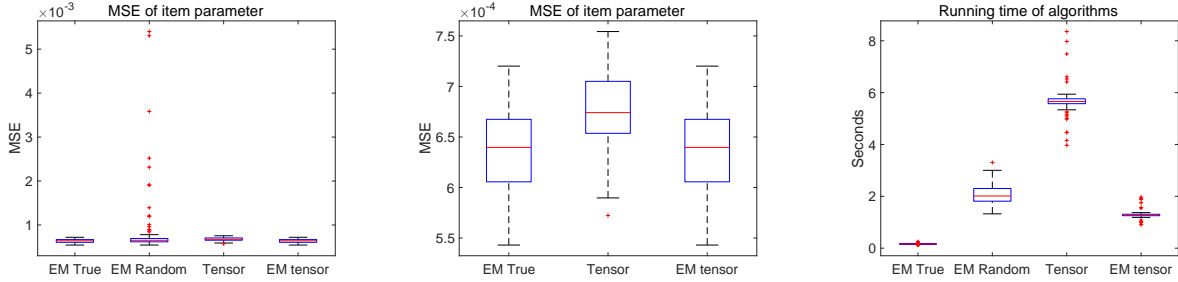


(b) MSE without EM-random



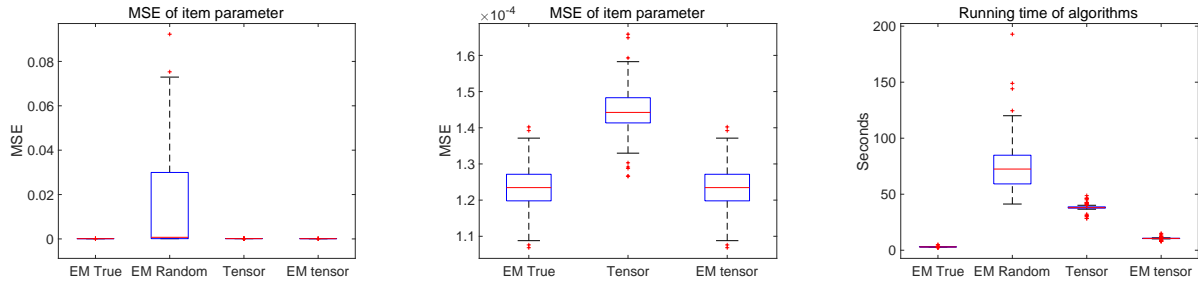
(c) Running time of the algorithms

Figure 3: Random-effect LCM, $N = 10000, J = 200, L = 10$, item parameters $\in \{0.2, 0.4, 0.6, 0.8\}$



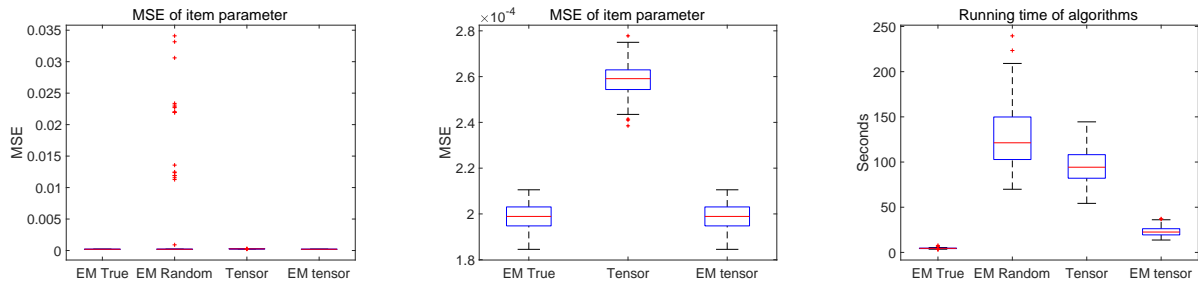
(a) MSE of item parameters (b) MSE without EM-random (c) Running time of the algorithms

Figure 4: Fixed-effect LCM, $N = 1000, J = 100, L = 5, \theta_{j,a} \in \{0.1, 0.2, 0.8, 0.9\}$



(a) MSE of item parameters (b) MSE without EM-random (c) Running time of the algorithms

Figure 5: Fixed-effect LCM, $N = 10000, J = 100, L = 10, \theta_{j,a} \in \{0.1, 0.2, 0.8, 0.9\}$



(a) MSE of item parameters (b) MSE without EM-random (c) Running time of the algorithms

Figure 6: Fixed-effect LCM, $N = 10000, J = 200, L = 10$, item parameters $\in \{0.2, 0.4, 0.6, 0.8\}$

From the boxplots in Figures 1–6 and those in Supplementary Material, we can see that for each setting, the MSE of the tensor-EM method is almost the same as that of the EM-true method. The EM-random method sometimes yields local maximizer of log-likelihood function and thus its estimates have a large MSE. The tensor estimates alone have a larger MSE compared with the

tensor-EM estimates but are more stable than the EM-random estimates. Comparing the running time of different algorithms, we can find that the tensor-EM method is computationally efficient, only second to the performance of EM-true with true parameters as initials values. On the other hand, the EM-random method can be computationally intensive because it needs more steps to converge.

The sample size N , number of classes L and number of items J all affect the accuracy and running time of the methods examined. As the sample size N increases, the accuracy of the methods is improved while they all need more time. As the number of classes L increases, the MSE of EM-tensor estimates also becomes larger because we have more parameters to estimate. As the number of items J increases, the accuracy of EM-tensor remains comparable to EM-true while the accuracy of tensor method alone is improved. The running time increases as J, L becomes large. When the item parameters are generated in $\{0.1, 0.2, 0.8, 0.9\}$, the signal strength is strong and the estimates have smaller MSE compared with cases where item parameters are generated from $\{0.2, 0.4, 0.6, 0.8\}$ where the signal strength is weaker. We also note that the random-effect and fixed-effect LCMs with the same N, J, L and item parameters share similar orders of MSEs.

5.2 Verification of Clustering Consistency

In this subsection, we empirically verify Theorem 3 in fixed-effect LCMs with diverging N and J . Specifically, we consider fixed-effect LCM with $L = 5$ classes. We let J increase from 20 to 100 by 10 and set $N = 10J$ in all the simulations. Item parameters are generated uniformly from either $\{0.1, 0.2, 0.8, 0.9\}$ or $\{0.2, 0.4, 0.6, 0.8\}$ and latent class assignments \mathbf{z} are sampled uniformly over $[L]$. After item parameters and latent class assignments are generated, we generate response \mathbf{R} accordingly. Since we have shown that tensor-EM method has good performance in Section 5.1, we then apply tensor-EM method to obtain the joint MLE $(\hat{\boldsymbol{\theta}}, \hat{\mathbf{Z}})$. The error of the estimated latent class assignments $\hat{\mathbf{Z}}$ is evaluated and the number of incorrect assignments $N_e(\hat{\mathbf{z}})$ defined in (13) is computed for each replication. This process of generating \mathbf{R} , estimating \mathbf{Z} and evaluating error is replicated 100 times and the boxplots of error rate $N_e(\hat{\mathbf{z}})/N$ are shown in Figure 7. According to these plots, the error rate of the estimated latent class membership \mathbf{z} decays to zero as N, J

increases. Again in the strong signal setting where $\theta_{j,a} \in \{0.1, 0.2, 0.8, 0.9\}$ the error rate converges to zero faster.

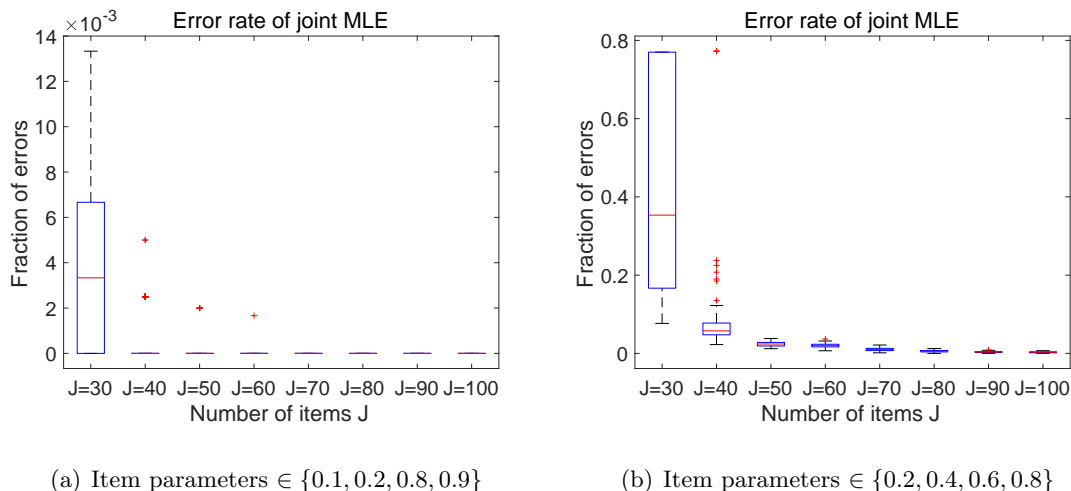


Figure 7: Error rate of joint MLE in latent class assignments versus number of items J

5.3 Performance of GIC in Selecting Number of Classes

We consider the accuracy of GIC in selecting L , which needs to be estimated in practice. The settings we consider are the same as in Section 5.1. The performance of GIC to select the number of classes in the random-effect LCM and the fixed-effect LCM are reported in Table 1. For settings with the true number of classes L being five, we let the candidate set of L to choose from be $\{2, 3, 4, 5, 6, 7\}$; while for settings with the true L being ten, we let the candidate set of L be $\{7, 8, 9, 10, 11, 12\}$. We see that for all these settings GIC_1 can always select the correct number of classes. And for most of the settings GIC_2 can choose the right model. The only setting where GIC_2 performs not so well is random-effect LCM with $N = 1000, J = 100, L = 10, \theta_{j,a} \in \{0.2, 0.4, 0.6, 0.8\}$. In general, both GIC_1 and GIC_2 enjoy desirable performance in selecting the correct number of classes.

6 Real Data Analysis

In this section we apply the proposed method to IPIP HEXACO equivalent scales data. The raw data can be found on https://openpsychometrics.org/_rawdata/. The data contains 22786 samples and 240 items. The details of the personality measured by each item are specified at

Signal strength	N	J	L	Random-effect		Fixed-effect	
				GIC ₁	GIC ₂	GIC ₁	GIC ₁
$\theta_{j,a} \in \{0.1, 0.2, 0.8, 0.9\}$	1000	100	5	1.00	1.00	1.00	1.00
			10	1.00	1.00	1.00	1.00
		200	5	1.00	1.00	1.00	1.00
			10	1.00	1.00	1.00	1.00
	10000	100	5	1.00	1.00	1.00	1.00
			10	1.00	1.00	1.00	1.00
		200	5	1.00	1.00	1.00	1.00
			10	1.00	1.00	1.00	1.00
	20000	100	5	1.00	1.00	1.00	1.00
			10	1.00	1.00	1.00	1.00
		200	5	1.00	1.00	1.00	1.00
			10	1.00	1.00	1.00	1.00
$\theta_{j,a} \in \{0.2, 0.4, 0.6, 0.8\}$	1000	100	5	1.00	1.00	1.00	1.00
			10	1.00	0.77	1.00	1.00
		200	5	1.00	1.00	1.00	1.00
			10	1.00	0.99	1.00	1.00
	10000	100	5	1.00	1.00	1.00	1.00
			10	1.00	1.00	1.00	1.00
		200	5	1.00	1.00	1.00	1.00
			10	1.00	1.00	1.00	1.00
	20000	100	5	1.00	1.00	1.00	1.00
			10	1.00	1.00	1.00	1.00
		200	5	1.00	1.00	1.00	1.00
			10	1.00	1.00	1.00	1.00

Table 1: The fraction of correctly selecting the number of classes

https://ipip.ori.org/newhexaco_pi_key.htm, including whether a positive answer to an item implies a high-level possession of a particular personality. There are six personalities (Honesty-Humility, Emotionality, Extraversion, Agreeableness, Conscientiousness and Openness to Experience) in total and 40 items measuring each one of them. Since all items are rated on a seven point scale, we convert them to binary in the following way. For those items positively related to a personality (marked by a '+' on the website), 5 (slightly agree), 6 (agree) and 7 (strongly agree) will be regarded as positive response and the answers will be set to 1. Otherwise they are set to 0. For those

items negatively correlated with a quality (marked by a ‘-’ on the website), 1 (strongly disagree), 2 (disagree) and 3 (slightly disagree) will be regarded as positive response and the answers will be set to 1. Otherwise they are set to 0.

After transforming the data, we consider fitting a random-effect LCM for the data. We apply the GIC method to selecting the number of latent classes. According to Figure 8, the GIC criterion selects eight classes for the data. Note that the real data may not strictly follow the model setup and the tensor-EM estimates may vary, depending on the initial values of the robust tensor power method in Algorithm 1. We further run the proposed method multiple times and find that fitting a model with fewer classes yields a higher GIC than the model fitted with eight classes shown in the Figure 8. Although a model with more classes (over eight classes) might have a slightly smaller GIC value in some cases, there is always at least one component in the estimated proportion vector $\hat{\mathbf{p}}$ being fairly small (smaller than 0.001); thus the corresponding latent class can be neglected for better interpretability and parsimony, and it is still reasonable to select eight classes.

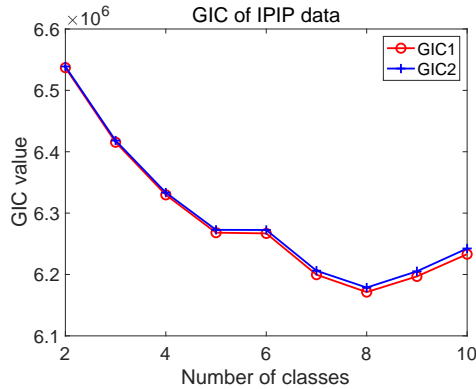


Figure 8: GIC of models with different number of classes

We consider the fitted eight-class model in Figure 8. After obtaining the item parameters $\hat{\boldsymbol{\theta}} \in \mathbb{R}^{240 \times 8}$, we pool the 40 item parameters corresponding to each of six personalities for each class. To be more concrete, for each l -th class and k -th personality, we calculate the mean of item parameters in the set $\{\hat{\theta}_{j,l}, 40(k-1)+1 \leq j \leq 40k\}$ and obtain $\bar{\theta}_{k,l} = \sum_{j=40(k-1)+1}^{40k} \hat{\theta}_{j,l} / 40$. These personality-level item parameters are collected in a matrix $\bar{\boldsymbol{\theta}} \in \mathbb{R}^{6 \times 8}$. Then each entry $\bar{\theta}_{k,l}$ is compared with certain threshold to decide whether it shows a high level possession of k -th

personality for l -th class. The results are shown in Figure 9. The left panel is based on the absolute value and the right based on quantiles in $\widehat{\boldsymbol{\theta}}$. In the left panel we compare $\bar{\theta}_{k,l}$ with 0.4, 0.6 to decide the level of k -th personality of l -th class. If $\bar{\theta}_{k,l} < 0.4$, it is of low level (marked with blue). If $0.4 \leq \bar{\theta}_{k,l} < 0.6$, then it is of medium level (marked with green). Otherwise it is said to be high level (marked with yellow). In the right panel we use some data-dependent threshold. We define

$$\widehat{\theta}_{k,\alpha} = \text{the } 100\alpha\text{th percentile of } \{\widehat{\theta}_{j,l}, 40(k-1) + 1 \leq j \leq 40k, 1 \leq l \leq 8\}$$

and if $\bar{\theta}_{k,l} < \widehat{\theta}_{k,0.4}$ we think the k -th personality of l -th class is of low level (blue). If $\widehat{\theta}_{k,0.4} \leq \bar{\theta}_{k,l} < \widehat{\theta}_{k,0.6}$, it is said to be of medium level (green). Otherwise it is said to be of high level (yellow). So the value of $\bar{\theta}_{k,l}$ decides the (k, l) -th square in the figure.

The estimated population proportion vector is $\mathbf{p} = (0.1027, 0.1534, 0.1175, 0.1118, 0.1010, 0.1519, 0.1596, 0.1019)$, which shows a relatively even distribution over the eight latent classes. According to the results, the first class is an all-round developed class and tend to have all these personalities at a high level while the last class tends to have a relatively lower level of all personalities. Similar interpretation can be derived for other latent classes. All latent classes tend to be somewhat “open to experience” according to the left panel of Figure 9.

7 Discussion

This paper investigates the computation and theory for large-scale latent class models. In terms of computation, commonly used likelihood-based methods (e.g. EM algorithm) suffer from slow convergence rate and potential convergence to local optima under poor initializations. Recent developments in tensor decomposition and its applications provide a computationally efficient moment-based method to estimate the parameters. However, such tensor method is based on low-order moments of the observed variables rather than the entire likelihood function. Hence it is not statistically efficient and generally requires a large number of samples to ensure the accuracy of estimates. In this work, we propose a two-stage tensor-EM estimation pipeline which combines these two methods. Simulation studies empirically show the proposed procedure is both computationally efficient and statistically accurate. Further, we also theoretically establish the clustering consistency

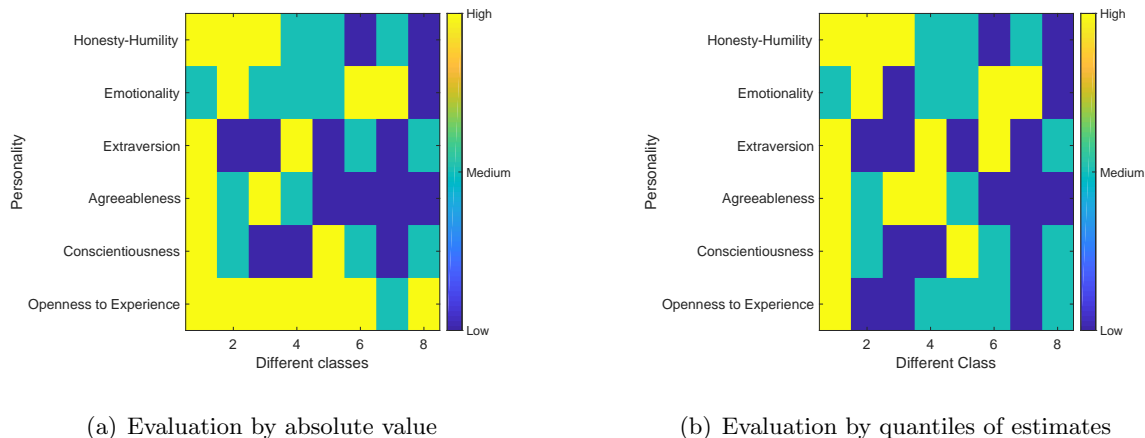


Figure 9: Evaluation of personality level for different classes. In the left panel we compare the mean of 40 item parameters of a personality for each class with 0.4 and 0.6 to decide its level. In the right panel we compare the mean of item parameters with 40% and 60% quantile of all the 320 item parameters in all classes measuring the same personality to decide its level. Yellow, green, blue represent a high, medium, low level of the personality, respectively.

of large-scale latent class analysis where sample size N and number of items J both go to infinity.

We also note that it is also possible to find similar tensor structures in more complicated latent structure models, for example, the diagnostic classification models or cognitive diagnostic models (CDMs) (Rupp and Templin, 2008; von Davier and Lee, 2019). This is because the low-order moments constructed in and exploited by the tensor power method here (also see Anandkumar et al., 2014) are essentially resulting from the local independence assumption in LCMs; that is, the observed variables are conditionally independent given the latent variable. Since CDMs can be viewed as extensions of LCMs where the local independence assumption also holds, the same tensor power method used here may also be used to find rough estimates of parameters in a CDM. However, CDMs also have a unique feature, the Q -matrix (Tatsuoka, 1983), which induces complicated parameter constraints on top of a latent class model. Thus a plain tensor power method for unrestricted LCMs would not give estimates that satisfy the equality constraints under a Q -matrix. How to develop an efficient estimation procedure for CDMs by integrating the tensor method is an interesting question left for future investigation.

Acknowledgements

This research was partially supported by National Science Foundation CAREER SES-1846747 and Institute of Education Sciences R305D200015. This research was also partially supported by grants R01ES027498 and R01ES028804 of the National Institutes of Environmental Health Sciences of the United States National Institutes of Health. This project has also received funding from the European Research Council under the European Union’s Horizon 2020 research and innovation program (grant agreement No 856506).

References

- Allman, E. S., Matias, C., and Rhodes, J. A. (2009). Identifiability of parameters in latent structure models with many observed variables. *The Annals of Statistics*, 37(6A):3099–3132.
- Anandkumar, A., Foster, D. P., Hsu, D. J., Kakade, S. M., and Liu, Y.-K. (2012). A spectral algorithm for latent dirichlet allocation. In *Advances in Neural Information Processing Systems*, pages 917–925.
- Anandkumar, A., Ge, R., Hsu, D., Kakade, S. M., and Telgarsky, M. (2014). Tensor decompositions for learning latent variable models. *The Journal of Machine Learning Research*, 15(1):2773–2832.
- Balakrishnan, S., Wainwright, M. J., and Yu, B. (2017). Statistical guarantees for the EM algorithm: From population to sample-based analysis. *The Annals of Statistics*, 45(1):77–120.
- Bandeen-Roche, K., Miglioretti, D. L., Zeger, S. L., and Rathouz, P. J. (1997). Latent variable regression for multiple discrete outcomes. *Journal of the American Statistical Association*, 92(440):1375–1386.
- Bucholz, K., Hesselbrock, V., Heath, A., Kramer, J., and Schuckit, M. (2000). A latent class analysis of antisocial personality disorder symptom data from a multi-centre family study of alcoholism. *Addiction*, 95(4):553–567.

- Celeux, G. and Govaert, G. (1992). A classification EM algorithm for clustering and two stochastic versions. *Computational statistics & Data analysis*, 14(3):315–332.
- Chaganty, A. T. and Liang, P. (2013). Spectral experts for estimating mixtures of linear regressions. In *International Conference on Machine Learning*, pages 1040–1048. PMLR.
- Chen, Y., Li, X., Liu, J., and Ying, Z. (2017). Regularized latent class analysis with application in cognitive diagnosis. *Psychometrika*, 82(3):660–692.
- Collins, L. M. and Lanza, S. T. (2009). *Latent class and latent transition analysis: With applications in the social, behavioral, and health sciences*, volume 718. John Wiley & Sons.
- De, L., De Moor, B., and Vandewalle, J. (2000). On the best rank-1 and rank- (R_1, R_2, \dots, R_n) approximation of higher-order tensors. *SIAM J. Matrix Anal. Appl.*, 21(4):1324–1342.
- De Lathauwer, L. and De Moor, B. (1998). From matrix to tensor: Multilinear algebra and signal processing. In *Institute of mathematics and its applications conference series*, volume 67, pages 1–16. Citeseer.
- Dean, N. and Raftery, A. E. (2010). Latent class analysis variable selection. *Annals of the Institute of Statistical Mathematics*, 62(1):11.
- Dempster, A. P., Laird, N. M., and Rubin, D. B. (1977). Maximum likelihood from incomplete data via the EM algorithm. *Journal of the Royal Statistical Society: Series B (Methodological)*, 39(1):1–22.
- Dunn, K. M., Jordan, K., and Croft, P. R. (2006). Characterizing the course of low back pain: a latent class analysis. *American journal of epidemiology*, 163(8):754–761.
- Fan, Y. and Tang, C. Y. (2013). Tuning parameter selection in high dimensional penalized likelihood. *Journal of the Royal Statistical Society: Series B (Statistical Methodology)*, 75(3):531–552.
- Goodman, L. A. (1974). Exploratory latent structure analysis using both identifiable and unidentifiable models. *Biometrika*, 61(2):215–231.

- Gu, Y. and Xu, G. (2020). A joint MLE approach to large-scale structured latent attribute analysis. *arXiv preprint arXiv:2009.04096*.
- Hagenaars, J. A. and McCutcheon, A. L. (2002). *Applied latent class analysis*. Cambridge University Press.
- Harshman, R. A. (1970). *Foundations of the PARAFAC procedure: Models and conditions for an “explanatory” multimodal factor analysis*. University of California at Los Angeles Los Angeles, CA.
- Hitchcock, F. L. (1927). The expression of a tensor or a polyadic as a sum of products. *Journal of Mathematics and Physics*, 6(1-4):164–189.
- Hsu, D. and Kakade, S. M. (2013). Learning mixtures of spherical Gaussians: moment methods and spectral decompositions. In *Proceedings of the 4th conference on Innovations in Theoretical Computer Science*, pages 11–20. ACM.
- Keel, P. K., Fichter, M., Quadflieg, N., Bulik, C. M., Baxter, M. G., Thornton, L., Halmi, K. A., Kaplan, A. S., Strober, M., Woodside, D. B., et al. (2004). Application of a latent class analysis to empirically define eatingdisorder phenotypes. *Archives of General Psychiatry*, 61(2):192–200.
- Kolda, T. G. and Bader, B. W. (2009). Tensor decompositions and applications. *SIAM review*, 51(3):455–500.
- Kruskal, J. B. (1976). More factors than subjects, tests and treatments: an indeterminacy theorem for canonical decomposition and individual differences scaling. *Psychometrika*, 41(3):281–293.
- Lanza, S. T. and Rhoades, B. L. (2013). Latent class analysis: an alternative perspective on subgroup analysis in prevention and treatment. *Prevention Science*, 14(2):157–168.
- Lazarsfeld, P. F. and Henry, N. W. (1968). *Latent structure analysis*. Houghton Mifflin Co.
- McCullagh, P. (2018). *Tensor Methods in Statistics: Monographs on Statistics and Applied Probability*. Chapman and Hall/CRC.
- McLachlan, G. and Peel, D. (2004). *Finite mixture models*. John Wiley & Sons.

- Neyman, J. and Scott, E. L. (1948). Consistent estimates based on partially consistent observations. *Econometrica: Journal of the Econometric Society*, pages 1–32.
- Nishii, R. (1984). Asymptotic properties of criteria for selection of variables in multiple regression. *The Annals of Statistics*, pages 758–765.
- Nylund, K. L., Asparouhov, T., and Muthén, B. O. (2007). Deciding on the number of classes in latent class analysis and growth mixture modeling: A Monte Carlo simulation study. *Structural equation modeling: A multidisciplinary Journal*, 14(4):535–569.
- Rupp, A. A. and Templin, J. L. (2008). Unique characteristics of diagnostic classification models: A comprehensive review of the current state-of-the-art. *Measurement*, 6(4):219–262.
- Schwarz, G. (1978). Estimating the dimension of a model. *The Annals of Statistics*, 6(2):461–464.
- Smilde, A., Bro, R., and Geladi, P. (2005). *Multi-way analysis: applications in the chemical sciences*. John Wiley & Sons.
- Tatsuoka, K. K. (1983). Rule space: An approach for dealing with misconceptions based on item response theory. *Journal of Educational Measurement*, pages 345–354.
- Tucker, L. R. (1964). The extension of factor analysis to three-dimensional matrices. *Contributions to Mathematical Psychology*, 110119.
- Tucker, L. R. (1966). Some mathematical notes on three-mode factor analysis. *Psychometrika*, 31(3):279–311.
- Vermunt, J. K. (2010). Latent class modeling with covariates: Two improved three-step approaches. *Political analysis*, pages 450–469.
- von Davier, M. and Lee, Y.-S. (2019). Handbook of diagnostic classification models. Cham: Springer International Publishing.
- Wang, M. and Hanges, P. J. (2011). Latent class procedures: Applications to organizational research. *Organizational Research Methods*, 14(1):24–31.

Xu, G. (2017). Identifiability of restricted latent class models with binary responses. *The Annals of Statistics*, 45(2):675–707.

Zhang, Y., Chen, X., Zhou, D., and Jordan, M. I. (2014). Spectral methods meet EM: A provably optimal algorithm for crowdsourcing. *arXiv preprint arXiv:1406.3824*.

Appendices

In this appendices, the proof of Theorem 3 (clustering consistency) is presented in Appendix 1. In Appendix 2, more simulation results are provided to show the good performance of the proposed EM-tensor method.

Appendix 1: Proof of Theorem 3

Outline of proof idea. The proof follows the following 8 steps.

Step 1: Express $\ell(\mathbf{R}; \mathbf{Z}) - \bar{\ell}(\mathbf{Z})$ in terms of $\sum_a n_a \sum_j D(\hat{\theta}_{j,a} \parallel \bar{\theta}_{j,a}) + X - \mathbb{E}(X)$, where X is a random variable depending on \mathbf{R} and $\bar{\boldsymbol{\theta}}^{(\mathbf{Z})}$ under \mathbf{Z} , and $n_a = \sum_{i=1}^N Z_{i,a}$.

Step 2: Bound the first term $\sum_j \sum_a n_{j,a} D(\hat{\theta}_{j,a} \parallel \bar{\theta}_{j,a})$ in the above display uniformly over all possible \mathbf{Z} .

Step 3: Bound the second term $X - \mathbb{E}(X)$ using possibly Bernstein type inequality. Combine this and Step 2 to obtain a bound for $\sup_{\mathbf{Z}} |\ell(\mathbf{R}; \mathbf{Z}) - \bar{\ell}(\mathbf{Z})|$.

Step 4: (Denote the true latent class memberships by \mathbf{Z}^0 and the those maximizing the likelihood by $\hat{\mathbf{Z}}$.) Establish $\bar{\ell}(\mathbf{Z}^0) \geq \bar{\ell}(\mathbf{Z})$ for all \mathbf{Z} . Use triangle inequality to upper-bound the non-negative quantity $\bar{\ell}(\mathbf{Z}^0) - \bar{\ell}(\hat{\mathbf{Z}})$.

$$0 \leq \bar{\ell}(\mathbf{Z}^0) - \bar{\ell}(\hat{\mathbf{Z}}) \leq [\bar{\ell}(\mathbf{Z}^0) - \ell(\mathbf{R}; \mathbf{Z}^0)] + [\ell(\mathbf{R}; \mathbf{Z}^0) - \ell(\mathbf{R}; \hat{\mathbf{Z}})] + [\ell(\mathbf{R}; \hat{\mathbf{Z}}) - \bar{\ell}(\hat{\mathbf{Z}})]$$

Since in the above display the middle group of terms $[\ell(\mathbf{R}; \mathbf{Z}^0) - \ell(\mathbf{R}; \hat{\mathbf{Z}})] \leq 0$, we have $0 \leq \bar{\ell}(\mathbf{Z}^0) - \bar{\ell}(\hat{\mathbf{Z}}) \leq 2 \sup_{\mathbf{Z}} |\ell(\mathbf{R}; \mathbf{Z}) - \bar{\ell}(\mathbf{Z})|$.

Step 5: Introduce the notion of partitions and generalize $\bar{\ell}(\mathbf{Z})$ to $\bar{\ell}(\Pi)$.

Step 6: Show that a refined partition increases $\bar{\ell}(\cdot)$. To be concrete, let Π^* be a refined partition of Π , then we have $\bar{\ell}(\Pi^*) \geq \bar{\ell}(\Pi)$.

Step 7: Show that for any latent class assignment \mathbf{Z} , we can find a partition Π^* that refines $\Pi^{\mathbf{Z}}$ and $\bar{\ell}(\mathbf{Z}^0) - \bar{\ell}(\Pi^*) \geq \frac{1}{2} J \beta_J^2 N_e(z)$.

Step 8: Apply results in step 6 and step 7 to MLE \hat{z} , we have

$$\text{bound in step 4} \geq \bar{\ell}(\mathbf{Z}^0) - \bar{\ell}(\Pi^{\hat{\mathbf{Z}}}) \geq \bar{\ell}(\mathbf{Z}^0) - \bar{\ell}(\Pi^*) \geq \frac{1}{2} J \beta_J^2 N_e(\hat{z}).$$

Now we formally begin the proof of Theorem 3 in the above several steps. In derivations below we abbreviate $\bar{\theta}^{(\mathbf{Z})}$ as $\bar{\theta}$ and $\hat{\theta}^{(\mathbf{Z})}$ as $\hat{\theta}$ to simplify notations.

Step 1. Define $D(p||q) = p \log(p/q) + (1-p) \log((1-p)/(1-q))$, the Kullback-Leibler divergence of a Bernoulli distribution with parameter p from that with parameter q . In this step we prove a lemma as follows.

Lemma 1. *Let $(R_{i,j}; 1 \leq N, 1 \leq J)$ denote independent Bernoulli trials with parameters $(P_{i,j}; 1 \leq N, 1 \leq J)$. Under a general latent class model, given an arbitrary \mathbf{Z} , there is*

$$\begin{aligned} & \sup_{\boldsymbol{\theta}} \ell(\mathbf{R}; \mathbf{Z}, \boldsymbol{\theta}) - \sup_{\boldsymbol{\theta}} \mathbb{E}[\ell(\mathbf{R}; \mathbf{Z}, \boldsymbol{\theta})] \\ &= \sum_{a=1}^L n_a \sum_j D(\hat{\theta}_{j,a} || \bar{\theta}_{j,a}) + \sum_i \sum_j (R_{i,j} - P_{i,j}) \log \left(\frac{\bar{\theta}_{j,z_i}}{1 - \bar{\theta}_{j,z_i}} \right) \\ &= \sum_{a=1}^L n_a \sum_j D(\hat{\theta}_{j,a} || \bar{\theta}_{j,a}) + X - \mathbb{E}X, \end{aligned} \tag{15}$$

where $X = \sum_i \sum_j R_{i,j} \log \left(\frac{\bar{\theta}_{j,z_i}}{1 - \bar{\theta}_{j,z_i}} \right)$ is random variable depending on \mathbf{Z} and

$$\hat{\theta}_{j,a} = \frac{\sum_i Z_{i,a} R_{i,j}}{\sum_i Z_{i,a}}, \quad \bar{\theta}_{j,a} = \frac{\sum_i Z_{i,a} P_{i,j}}{\sum_i Z_{i,a}} \tag{16}$$

Given a fixed \mathbf{Z} , denote $n_a^{(\mathbf{Z})} = \sum_{i=1}^N Z_{i,a}$. The maximizing properties of $\hat{\theta}_{j,a}$ and $\bar{\theta}_{j,a}$ in 16 imply that

$$n_a \hat{\theta}_{j,a} = \sum_i Z_{i,a} R_{i,j}, \quad n_a \bar{\theta}_{j,a} = \sum_i Z_{i,a} P_{i,j}. \tag{17}$$

Using (17), we have the following,

$$\begin{aligned} & \ell(\mathbf{R}; \mathbf{Z}) - \bar{\ell}(\mathbf{Z}) \\ &= \sum_i \sum_j \sum_{a=1}^L Z_{i,a} [R_{i,j} \log \hat{\theta}_{j,a} + (1 - R_{i,j}) \log(1 - \hat{\theta}_{j,a})] \\ & \quad - \sum_i \sum_j \sum_{a=1}^L Z_{i,a} [P_{i,j} \log \bar{\theta}_{j,a} + (1 - P_{i,j}) \log(1 - \bar{\theta}_{j,a})] \\ &= \sum_j \sum_{a=1}^L n_a [\hat{\theta}_{j,a} \log \hat{\theta}_{j,a} + (1 - \hat{\theta}_{j,a}) \log(1 - \hat{\theta}_{j,a})] - \sum_j \sum_{a=1}^L n_a [\bar{\theta}_{j,a} \log \bar{\theta}_{j,a} + (1 - \bar{\theta}_{j,a}) \log(1 - \bar{\theta}_{j,a})] \\ &= \sum_j \sum_{a=1}^L \left\{ n_a [\hat{\theta}_{j,a} \log \hat{\theta}_{j,a} + (1 - \hat{\theta}_{j,a}) \log(1 - \hat{\theta}_{j,a})] - n_a [\bar{\theta}_{j,a} \log \bar{\theta}_{j,a} + (1 - \bar{\theta}_{j,a}) \log(1 - \bar{\theta}_{j,a})] \right\} \end{aligned}$$

$$\begin{aligned}
& + \sum_j \sum_{a=1}^L \left\{ n_a [\widehat{\theta}_{j,a} \log \bar{\theta}_{j,a} + (1 - \widehat{\theta}_{j,a}) \log(1 - \bar{\theta}_{j,a})] - n_a [\bar{\theta}_{j,a} \log \bar{\theta}_{j,a} + (1 - \bar{\theta}_{j,a}) \log(1 - \bar{\theta}_{j,a})] \right\} \\
& = \sum_{a=1}^L n_a \sum_j D(\widehat{\theta}_{j,a} \| \bar{\theta}_{j,a}) + \sum_i \sum_j \left\{ [R_{i,j} \log \bar{\theta}_{j,z_i} + (1 - R_{i,j}) \log(1 - \bar{\theta}_{j,z_i})] \right. \\
& \quad \left. - [P_{i,j} \log \bar{\theta}_{j,z_i} + (1 - P_{i,j}) \log(1 - \bar{\theta}_{j,z_i})] \right\} \\
& = \sum_{a=1}^L n_a \sum_j D(\widehat{\theta}_{j,a} \| \bar{\theta}_{j,a}) + \sum_i \sum_j R_{i,j} \log \left(\frac{\bar{\theta}_{j,z_i}}{1 - \bar{\theta}_{j,z_i}} \right) - \sum_i \sum_j P_{i,j} \log \left(\frac{\bar{\theta}_{j,z_i}}{1 - \bar{\theta}_{j,z_i}} \right).
\end{aligned}$$

Define the random variable

$$X = \sum_i \sum_j R_{i,j} \log(\bar{\theta}_{j,z_i} / (1 - \bar{\theta}_{j,z_i})), \quad (18)$$

then X depends on \mathbf{Z} and the above display becomes the summation of $\sum_{a=1}^L n_a \sum_j D(\widehat{\theta}_{j,a} \| \bar{\theta}_{j,a})$ and $X - \mathbb{E}[X]$. This establishes (15) in Lemma 1. In the following, we bound the first term $\sum_{a=1}^L n_a \sum_j D(\widehat{\theta}_{j,a} \| \bar{\theta}_{j,a})$ and the second term $X - \mathbb{E}[X]$ in the above display uniformly over all possible \mathbf{Z} , respectively in Step 2 and Step 3.

Step 2. In this step we prove the following theorem.

Theorem 4. *The following event happens with probability at least $1 - \delta$,*

$$\max_{\mathbf{Z}} \left\{ \sum_j \sum_a n_a D(\widehat{\theta}_{j,a}^{\mathbf{Z}} \| \bar{\theta}_{j,a}^{\mathbf{Z}}) \right\} < N \log L + JL \log \left(\frac{N}{L} + 1 \right) - \log \delta.$$

Given any fixed latent class memberships \mathbf{Z} , every $\widehat{\theta}_{j,a}$ is an average of n_a independent Bernoulli random variables $R_{1,j}, \dots, R_{N,j}$ with mean $\bar{\theta}_{j,a}$. We apply the Chernoff-Hoeffding theorem to obtain

$$\mathbb{P}(\widehat{\theta}_{j,a} \geq \bar{\theta}_{j,a} + t) \leq e^{-n_a D(\bar{\theta}_{j,a} + t \| \bar{\theta}_{j,a})}, \quad \mathbb{P}(\widehat{\theta}_{j,a} \leq \bar{\theta}_{j,a} - t) \leq e^{-n_a D(\bar{\theta}_{j,a} - t \| \bar{\theta}_{j,a})}. \quad (19)$$

Note that given a fixed \mathbf{Z} , each $\widehat{\theta}_{j,a}$ can take values only in the finite set $\{0, 1/n_a, 2/n_a, \dots, 1\}$ of cardinality $n_a + 1$. We denote this range of $\widehat{\theta}_{j,a}$ by $\widehat{\Theta}^{j,a}$. Then $\mathbb{P}(\widehat{\theta}_{j,a} = \vartheta) \leq \exp\{-n_a D(\vartheta \| \bar{\theta}_{j,a})\}$ for any $\vartheta \in \widehat{\Theta}^{j,a}$. Now consider the cardinality of the set $\widehat{\Theta}$ given \mathbf{Z} . Since for each of the $J \times L$ entries in $\widehat{\theta}$, $\widehat{\theta}_{j,a}$ can independently take on $n_a + 1$ different values, there is $|\widehat{\Theta}| = \prod_a (n_a + 1)^J$.

Considering the natural constraint $\sum_{a=1}^L n_a = N$, we have

$$|\widehat{\Theta}| = \left[\prod_{a=1}^L (n_a + 1) \right]^J \leq \left[\left(\frac{N}{L} + 1 \right)^L \right]^J. \quad (20)$$

Define $\widehat{\Theta}_\epsilon = \{\widehat{\boldsymbol{\theta}} \in \widehat{\Theta} : \sum_j \sum_a n_a D(\widehat{\theta}_{j,a} \|\bar{\theta}_{j,a}) \geq \epsilon\}$, then $\widehat{\Theta}_\epsilon \subseteq \widehat{\Theta}$. Note that the components of $\widehat{\boldsymbol{\theta}}$ depend on different components of $\{R_{i,j}, i \in [N], j \in [J]\}$ and thus are independent. We have

$$\begin{aligned}
& \mathbb{P}\left(\sum_{j=1}^J \sum_{a=1}^L n_a D(\widehat{\theta}_{j,a} \|\bar{\theta}_{j,a}) \geq \epsilon\right) \\
&= \sum_{\widehat{\boldsymbol{\theta}} \in \widehat{\Theta}_\epsilon} \mathbb{P}(\widehat{\boldsymbol{\theta}} = \widetilde{\boldsymbol{\theta}}) \\
&\leq \sum_{\widetilde{\boldsymbol{\theta}} \in \widehat{\Theta}_\epsilon} \prod_j \prod_a \exp\{-n_a D(\widetilde{\theta}_{j,a} \|\bar{\theta}_{j,a})\} \\
&\leq \sum_{\widetilde{\boldsymbol{\theta}} \in \widehat{\Theta}_\epsilon} \exp\{-n_a \sum_j \sum_a D(\widetilde{\theta}_{j,a} \|\bar{\theta}_{j,a})\} \\
&\leq \sum_{\widetilde{\boldsymbol{\theta}} \in \widehat{\Theta}_\epsilon} \exp\{-\epsilon\} \\
&\leq |\widehat{\Theta}_\epsilon| e^{-\epsilon} \leq |\widehat{\Theta}| e^{-\epsilon} \leq \left(\frac{N}{L} + 1\right)^{JL} e^{-\epsilon}.
\end{aligned}$$

The above result holds for fixed \mathbf{Z} , so applying a union bound over all the L^N possible assignment \mathbf{Z} , there is

$$\mathbb{P}\left(\max_{\mathbf{Z}} \left\{ \sum_j \sum_a n_a D(\widehat{\theta}_{j,a} \|\bar{\theta}_{j,a}) \right\} \geq \epsilon\right) \leq L^N \left(\frac{N}{L} + 1\right)^{JL} e^{-\epsilon}.$$

Now take $\delta = L^N \left(\frac{N}{L} + 1\right)^{JL} e^{-\epsilon}$, then $\epsilon = N \log L + JL \log\left(\frac{N}{L} + 1\right) - \log \delta$. Therefore the following event happens with probability at least $1 - \delta$,

$$\max_{\mathbf{Z}} \left\{ \sum_j \sum_a n_a D(\widehat{\theta}_{j,a} \|\bar{\theta}_{j,a}) \right\} < \epsilon = N \log L + JL \log\left(\frac{N}{L} + 1\right) - \log \delta.$$

This concludes the proof of Theorem 4.

Step 3. In this step we bound $|X - \mathbb{E}[X]|$, with X defined in (18). Denote $X_{i,j} = R_{i,j} \log(\bar{\theta}_{j,z_i} / (1 - \bar{\theta}_{j,z_i}))$, then $X = \sum_i \sum_j X_{i,j}$. Under Assumption 1, we have $|X_{i,j}| \leq d \log J$. Then we have $\sum_i \sum_j \mathbb{E}[X_{i,j}^2] \leq \sum_i \sum_j \mathbb{P}(R_{i,j} = 1) d^2 (\log J)^2 = d^2 \sum_i \sum_j P_{i,j} (\log J)^2 = d^2 M N J (\log J)^2$. Applying the Bernstein's inequality to the sum of independent bounded random variables, we have the following holds for any fixed \mathbf{Z} ,

$$\mathbb{P}(|X - \mathbb{E}[X]| \geq \epsilon) \leq 2 \exp \left\{ -\frac{(1/2)\epsilon^2}{\sum_i \sum_j \mathbb{E}[X_{i,j}^2] + (1/3)d \log(J)\epsilon} \right\}$$

$$\leq 2 \exp \left\{ -\frac{(1/2)\epsilon^2}{d^2 MNJ(\log J)^2 + (1/3)d \log(J)\epsilon} \right\}.$$

We next prove the following theorem.

Theorem 5. *Under the following scaling,*

$$\frac{J}{MN^{2(1-\xi)}} \rightarrow 0 \text{ for some small } \xi > 0, \quad MJ \rightarrow \infty, \quad (21)$$

we have

$$\frac{1}{NJ} \max_{\mathbf{Z}} |\ell(\mathbf{R}; \mathbf{Z}) - \bar{\ell}(\mathbf{Z})| = o_P \left(\frac{\sqrt{M}}{\sqrt{J}} (\log J)^{1+\eta} \right)$$

for any $\eta > 0$.

In this step we bound $|\ell(\mathbf{R}; \mathbf{Z}) - \bar{\ell}(\mathbf{Z})|$ uniformly over all the \mathbf{Z} . Combining the results of Step 2 and Step 3, since that there are L^N possible assignments of \mathbf{Z} , we apply the union bound to obtain

$$\begin{aligned} & \mathbb{P}(\max_{\mathbf{Z}} |\ell(\mathbf{R}; \mathbf{Z}) - \bar{\ell}(\mathbf{Z})| \geq 2\epsilon\delta_{NJ}) \\ & \leq L^N \mathbb{P} \left[\left\{ \sum_j \sum_a n_a D(\hat{\theta}_{j,a} \| \bar{\theta}_{j,a}) \geq \epsilon\delta_{NJ} \right\} \cup \{|X - \mathbb{E}[X]| \geq \epsilon\delta_{NJ}\} \right] \\ & \leq \exp \left\{ N \log L + JL \log \left(\frac{N}{L} + 1 \right) - \epsilon\delta_{NJ} \right\} \\ & \quad + 2 \exp \left\{ N \log L - \frac{(1/2)\epsilon^2 \delta_{NJ}^2}{d^2 MNJ(\log J)^2 + (1/3)d \log(J)\epsilon\delta_{NJ}} \right\}. \end{aligned} \quad (22)$$

In order for the second term on the right hand side of the above display to go to zero, the following of δ_{NJ} would suffice,

$$\delta_{NJ} = N \sqrt{MJ \log L} (\log J)^{1+\eta}. \quad (23)$$

for a small positive constant η . Then the right hand side of (22) goes to zero as N, J go large and hence the scaling of J described in the theorem yields $\mathbb{P}(\max_{\mathbf{Z}} |\ell(\mathbf{R}; \mathbf{Z}) - \bar{\ell}(\mathbf{Z})| \geq 2\epsilon\delta_{NJ}) = o(1)$, which implies

$$\frac{1}{NJ} \max_{\mathbf{Z}} |\ell(\mathbf{R}; \mathbf{Z}) - \bar{\ell}(\mathbf{Z})| = o_P \left(\frac{\sqrt{M \log L}}{\sqrt{J}} (\log J)^{1+\eta} \right) = o_P \left(\frac{\sqrt{M}}{\sqrt{J}} (\log J)^{1+\eta} \right). \quad (24)$$

This proves Theorem 5.

Step 4. Denote the true class assignments by \mathbf{Z}^0 . We first establish

$$\bar{\ell}(\mathbf{Z}^0) \geq \bar{\ell}(\mathbf{Z}), \quad \text{for all } \mathbf{Z}. \quad (25)$$

First note that $\theta_{j,z_i}^0 = P_{i,j}$, and

$$\bar{\theta}_{j,z_i} = \frac{\sum_{m=1}^N Z_{m,z_i}^0 P_{m,j}}{\sum_{m=1}^N Z_{m,z_i}^0} = \frac{\sum_{m=1}^N Z_{m,z_i}^0 P_{i,j}}{\sum_{m=1}^N Z_{m,z_i}^0} = P_{i,j}.$$

The difference $\bar{\ell}(\mathbf{Z}^0) - \bar{\ell}(\mathbf{Z})$ can be written as

$$\begin{aligned} \bar{\ell}(\mathbf{Z}^0) - \bar{\ell}(\mathbf{Z}) &= \sum_j \sum_i [P_{i,j} \log\left(\frac{\bar{\theta}_{j,z_i}^0}{\bar{\theta}_{j,z_i}^{\mathbf{Z}}}\right) + (1 - P_{i,j}) \log\left(\frac{1 - \bar{\theta}_{j,z_i}^0}{1 - \bar{\theta}_{j,z_i}^{\mathbf{Z}}}\right)] \\ &= \sum_j \sum_i [P_{i,j} \log\left(\frac{P_{i,j}}{\bar{\theta}_{j,z_i}^{\mathbf{Z}}}\right) + (1 - P_{i,j}) \log\left(\frac{1 - P_{i,j}}{1 - \bar{\theta}_{j,z_i}^{\mathbf{Z}}}\right)] = \sum_i \sum_j D(P_{i,j} \parallel \bar{\theta}_{j,z_i}^{\mathbf{Z}}) \geq 0, \end{aligned}$$

therefore establishing (25). Since the above holds for every \mathbf{Z} , it also holds for the maximum likelihood estimator $\hat{\mathbf{Z}}$. We further upper bound $\bar{\ell}(\mathbf{Z}^0) - \bar{\ell}(\mathbf{Z})$ from above as follows,

$$0 \leq \bar{\ell}(\mathbf{Z}^0) - \bar{\ell}(\hat{\mathbf{Z}}) \leq [\bar{\ell}(\mathbf{Z}^0) - \ell(\mathbf{R}; \mathbf{Z}^0)] + \underbrace{[\ell(\mathbf{R}; \mathbf{Z}^0) - \ell(\mathbf{R}; \hat{\mathbf{Z}})]}_{\leq 0} + [\ell(\mathbf{R}; \hat{\mathbf{Z}}) - \bar{\ell}(\hat{\mathbf{Z}})],$$

where $[\ell(\mathbf{R}; \mathbf{Z}^0) - \ell(\mathbf{R}; \hat{\mathbf{Z}})] \leq 0$ results from the definition of $\hat{\mathbf{Z}}$ as the MLE, that is \mathbf{Z} maximizes the $\ell(\mathbf{R}; \mathbf{Z}, \hat{\theta}^{\mathbf{Z}})$. Therefore

$$\begin{aligned} 0 \leq \bar{\ell}(\mathbf{Z}^0) - \bar{\ell}(\hat{\mathbf{Z}}) &\leq [\bar{\ell}(\mathbf{Z}^0) - \ell(\mathbf{R}; \mathbf{Z}^0)] + [\ell(\mathbf{R}; \hat{\mathbf{Z}}) - \bar{\ell}(\hat{\mathbf{Z}})] \\ &\leq 2 \sup_{\mathbf{Z}} |\bar{\ell}(\mathbf{Z}) - \ell(\mathbf{R}; \mathbf{Z})| \\ &= o_p(\delta_{NJ}). \end{aligned}$$

Step 5. To establish the consistency of MLE in clustering subjects into latent classes, we need to introduce the notion of partitions. First we observe that any latent class assignment \mathbf{Z} defines a partition on $[N]$ into T subsets (S_1, \dots, S_T) via mapping $\Pi^{\mathbf{Z}}$ from $[N]$ to $[T]$ such that for any subject we have $\theta_{j,z_i}^0 = \theta_{j,\Pi_i^{\mathbf{Z}}}^0$ for all j . We now generalize this notion. For any partition on $[N]$, define

$$\bar{\theta}_{j,a}^{\Pi} = \frac{1}{|S_a|} \sum_{i=1}^N \theta_{j,z_i}^0 I(i \in S_a) = \frac{1}{|S_a|} \sum_{i=1}^N P_{i,j} I(i \in S_a)$$

as the average over all i in the subset S_a indexed by $\Pi_i = a$. We then define generalization of $\bar{\ell}(\mathbf{Z})$

as

$$\bar{\ell}(\Pi) = \sum_i \sum_j [P_{i,j} \log(\bar{\theta}_{j,\Pi_i}^{\Pi}) + (1 - P_{i,j}) \log(1 - \bar{\theta}_{j,\Pi_i}^{\Pi})].$$

Note that $\bar{\theta}_{j,a}^{\Pi^{\mathbf{Z}}} = \bar{\theta}_{j,a}^{\mathbf{Z}}$ and hence $\bar{\ell}(\Pi^{\mathbf{Z}}) = \bar{\ell}(\mathbf{Z})$ when the partition $\Pi^{\mathbf{Z}}$ is induced by latent class assignment \mathbf{Z} .

We will proceed as follows: in step 6 we show a refined partition increases $\bar{\ell}(\cdot)$. We then construct a refined partition Π^* for every partition $\Pi^{\mathbf{Z}}$ induced by \mathbf{Z} and prove $\bar{\ell}(\mathbf{Z}^0) - \bar{\ell}(\Pi^*) \geq \frac{1}{2}N_e(z)\beta_J$ in step 7. Finally we apply the results to MLE $\widehat{\mathbf{Z}}$ and obtain the desired results in step 8.

Step 6. We prove the following lemma:

Lemma 2. *Let Π^* be a refinement of any partition Π of $[N]$, then we have $\bar{\ell}(\Pi^*) \geq \bar{\ell}(\Pi)$.*

Given $a \in [T^*]$ indexing S_a^* in Π^* , since $S_a^* \subseteq S_b$ for some S_b in Π , let $F(a)$ denote its index under Π (i.e. b). We have

$$\begin{aligned} \bar{\ell}(\Pi^*) &= \sum_{a=1}^{T^*} |S_a^*| \sum_{j=1}^J \left\{ \bar{\theta}_{j,a}^{\Pi^*} \log \bar{\theta}_{j,a}^{\Pi^*} + (1 - \bar{\theta}_{j,a}^{\Pi^*}) \log (1 - \bar{\theta}_{j,a}^{\Pi^*}) \right\} \\ &\geq \sum_{a=1}^{T^*} |S_a^*| \sum_{j=1}^J \left\{ \bar{\theta}_{j,a}^{\Pi^*} \log \bar{\theta}_{j,F(a)}^{\Pi} + (1 - \bar{\theta}_{j,a}^{\Pi^*}) \log (1 - \bar{\theta}_{j,F(a)}^{\Pi}) \right\} \\ &= \sum_{b=1}^T |S_b| \sum_{j=1}^J \left\{ \bar{\theta}_{j,b}^{\Pi} \log \bar{\theta}_{j,b}^{\Pi} + (1 - \bar{\theta}_{j,b}^{\Pi}) \log (1 - \bar{\theta}_{j,b}^{\Pi}) \right\} = \bar{\ell}(\Pi). \end{aligned}$$

The first equality is obtained by rewriting $\bar{\ell}(\Pi)$ in terms of subsets. The inequality follows from non-negativity of K-L distance. Then we combine terms in same class under Π and obtain the second equality.

Step 7. Now we prove a result on refinement.

Lemma 3. *For any latent class assignment \mathbf{Z} , there exists a partition Π^* that refines $\Pi^{\mathbf{Z}}$ and*

$$\bar{\ell}(\mathbf{Z}^0) - \bar{\ell}(\Pi^*) \geq \frac{1}{2}N_e(\mathbf{z})J\beta_J$$

For a given \mathbf{Z} , partition each latent class assigned by \mathbf{Z} into sub-classes according to true assignments \mathbf{Z}^0 of each sample. For each sample i_1 that is incorrectly assigned by \mathbf{Z} (by definition this means its true class under \mathbf{Z}^0 is not in the majority within its estimated class under \mathbf{Z}), we find another sample i_2 assigned to same class under \mathbf{Z} but i_1 and i_2 belong to different class under \mathbf{Z}^0 and make these two samples (i_1, i_2) a pair. We allow two misclassified samples to form a pair.

Note that since incorrectly assigned samples are not in the majority of that class, we can find a pair for each of them.

Here is a simple example. Suppose in one class of \mathbf{Z} , we have 7 samples and \mathbf{Z}^0 (true latent class assignments) assigns them as three sub-classes $\{1, 2, 3, 4\}, \{5, 6\}, \{7\}$. In this example samples indexed by 5,6 and 7 are misclassified. We can find pairs (4, 5), (6, 7).

The refined partition Π^* contains all such pairs and remaining correctly assigned samples in all classes assigned by \mathbf{Z} . So for the above example, the refined subset for that class is $\{1, 2, 3\}, \{4, 5\}, \{6, 7\}$. Let $e(\mathbf{z})$ be the set of incorrectly assigned sample. Clearly Π^* is a refinement and we have

$$\begin{aligned}\bar{\ell}(\mathbf{Z}^0) - \bar{\ell}(\Pi^*) &= \sum_i \sum_j D(P_{i,j} \| \bar{\theta}_{j,\Pi_i^*}^{\Pi^*}) \\ &\geq \sum_{i \in e(\mathbf{z})} \sum_j D(P_{i,j} \| \bar{\theta}_{j,\Pi_i^*}^{\Pi^*}) \\ &= \sum_{i \in e(\mathbf{z})} \sum_j D(P_{i,j} \| \frac{P_{i,j} + P_{i',j}}{2})\end{aligned}$$

where i and i' are in different classes under \mathbf{Z}^0 while in same subset under Π^* by definition. Apply Pinsker's inequality we have

$$\begin{aligned}D(P_{i,j} \| \frac{P_{i,j} + P_{i',j}}{2}) &\geq \frac{1}{2} \left[|P_{i,j} - \frac{P_{i,j} + P_{i',j}}{2}| + |1 - P_{i,j} - (1 - \frac{P_{i,j} + P_{i',j}}{2})| \right]^2 \\ &= \frac{1}{2} (P_{i,j} - P_{i',j})^2 \\ &= \frac{1}{2} (\theta_{j,z_i^0}^0 - \theta_{j,z_{i'}^0}^0)^2\end{aligned}$$

Hence we have

$$\begin{aligned}\bar{\ell}(\mathbf{Z}^0) - \bar{\ell}(\Pi^*) &\geq \sum_{i \in e(\mathbf{z})} \sum_j \frac{1}{2} (\theta_{j,z_i^0}^0 - \theta_{j,z_{i'}^0}^0)^2 \\ &\geq \sum_{i \in e(\mathbf{z})} \frac{1}{2} \|\boldsymbol{\theta}_{\cdot, z_i^0}^0 - \boldsymbol{\theta}_{\cdot, z_{i'}^0}^0\|^2 \\ &\geq \frac{1}{2} N_e(\mathbf{z}) J \beta_J\end{aligned}$$

Step 8. Apply Lemma 3 to MLE $\hat{\mathbf{z}}$, there exists a refinement of $\Pi^{\hat{\mathbf{z}}}$ denoted as Π^* such that

$$\bar{\ell}(\mathbf{Z}^0) - \bar{\ell}(\Pi^*) \geq \frac{1}{2} N_e(\mathbf{z}) J \beta_J$$

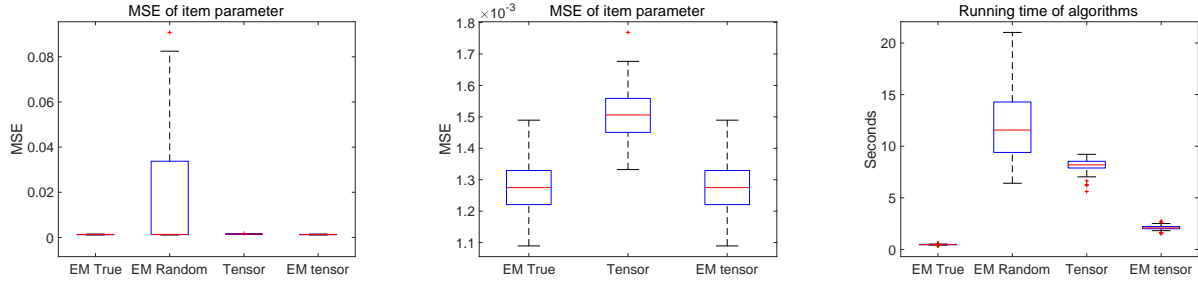
By Lemma 2 we have $\bar{\ell}(\Pi^*) \geq \bar{\ell}(\Pi^{\widehat{\mathbf{Z}}})$. So we conclude that

$$\begin{aligned} o_P(\delta_{NJ}) &= \bar{\ell}(\mathbf{Z}^0) - \bar{\ell}(\widehat{\mathbf{Z}}) \\ &\geq \bar{\ell}(\mathbf{Z}^0) - \bar{\ell}(\Pi^*) \\ &\geq \frac{1}{2}N_e(\mathbf{z})J\beta_J \end{aligned}$$

which completes the proof.

Appendix 2: More simulation results

First we present simulation results for random-effect LCM.

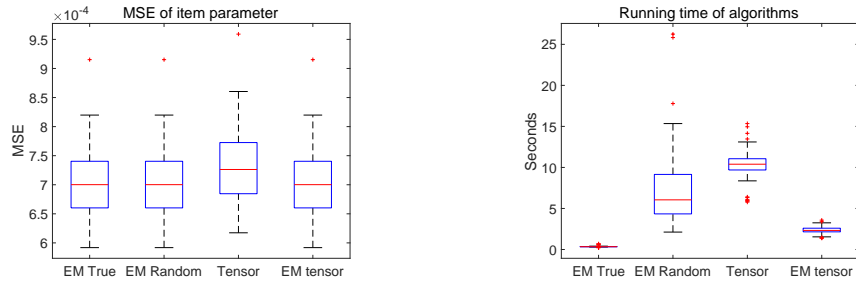


(a) MSE of item parameters

(b) MSE without EM-random

(c) Running time of the algorithms

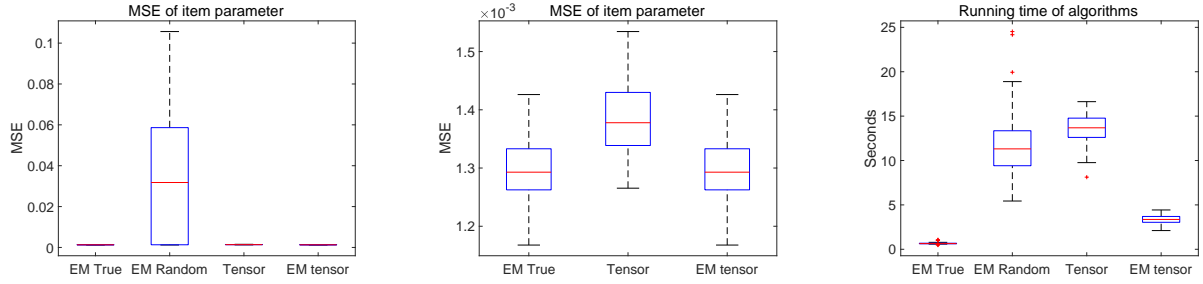
Figure 10: $N = 1000, J = 100, L = 10$, item parameters $\in \{0.1, 0.2, 0.8, 0.9\}$



(a) MSE of item parameters

(b) Running time of the algorithms

Figure 11: $N = 1000, J = 200, L = 5$, item parameters $\in \{0.1, 0.2, 0.8, 0.9\}$

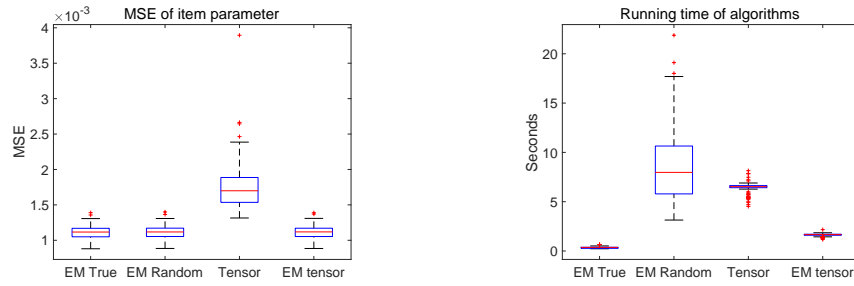


(a) MSE of item parameters

(b) MSE without EM-random

(c) Running time of the algorithms

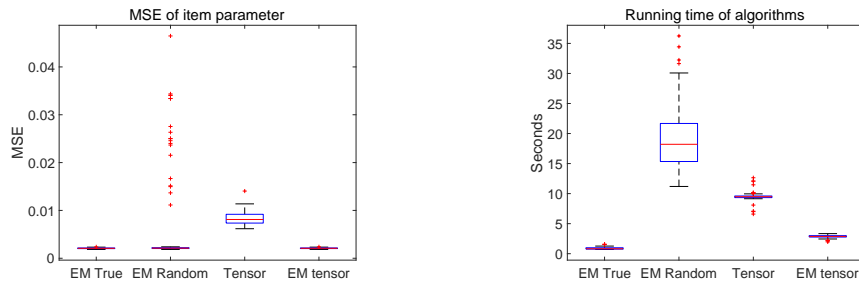
Figure 12: $N = 1000, J = 200, L = 10$, item parameters $\in \{0.1, 0.2, 0.8, 0.9\}$



(a) MSE of item parameters

(b) Running time of the algorithms

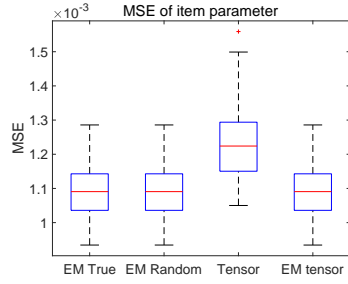
Figure 13: $N = 1000, J = 100, L = 5$, item parameters $\in \{0.2, 0.4, 0.6, 0.8\}$



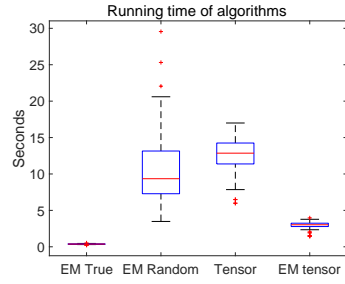
(a) MSE of item parameters

(b) Running time of the algorithms

Figure 14: $N = 1000, J = 100, L = 10$, item parameters $\in \{0.2, 0.4, 0.6, 0.8\}$

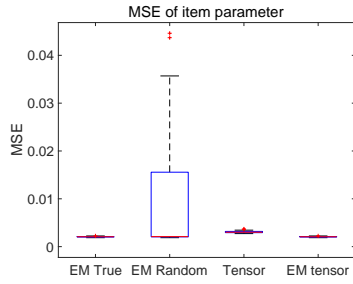


(a) MSE of item parameters

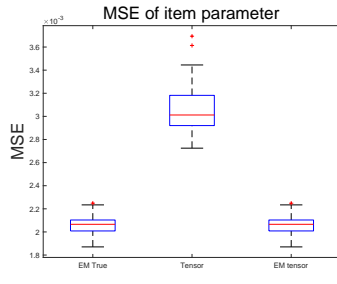


(b) Running time of the algorithms

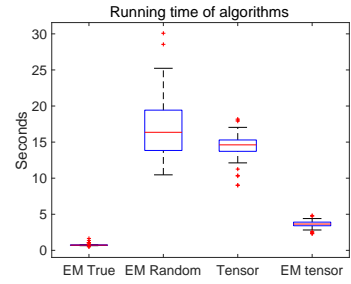
Figure 15: $N = 1000, J = 200, L = 5$, item parameters $\in \{0.2, 0.4, 0.6, 0.8\}$



(a) MSE of item parameters

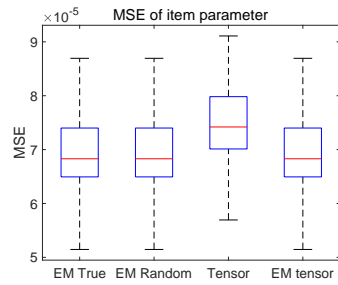


(b) MSE without EM-random

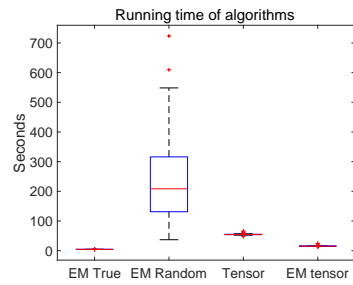


(c) Running time of the algorithms

Figure 16: $N = 1000, J = 200, L = 10$, item parameters $\in \{0.2, 0.4, 0.6, 0.8\}$

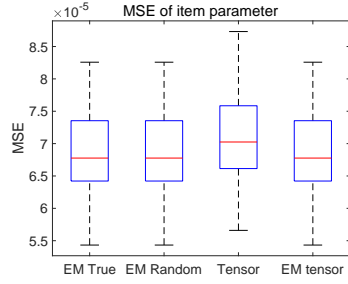


(a) MSE of item parameters

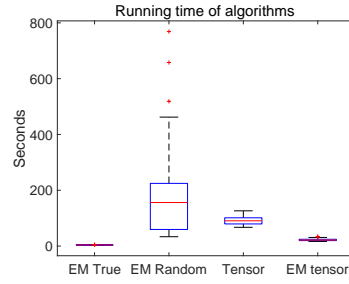


(b) Running time of the algorithms

Figure 17: $N = 10000, J = 100, L = 5$, item parameters $\in \{0.1, 0.2, 0.8, 0.9\}$

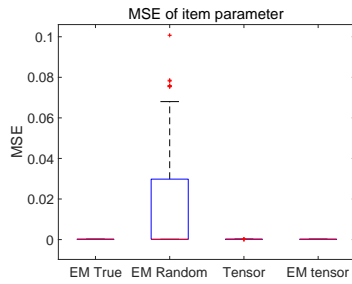


(a) MSE of item parameters

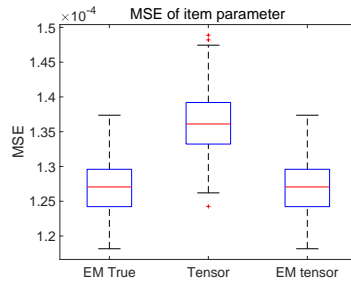


(b) Running time of the algorithms

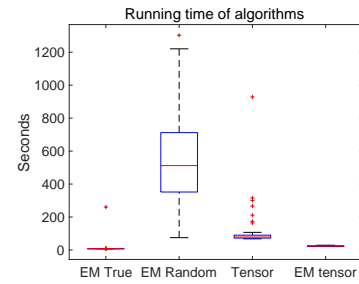
Figure 18: $N = 10000, J = 200, L = 5$, item parameters $\in \{0.1, 0.2, 0.8, 0.9\}$



(a) MSE of item parameters

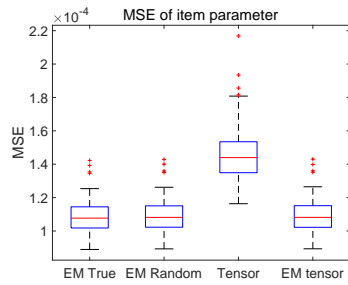


(b) MSE without EM-random

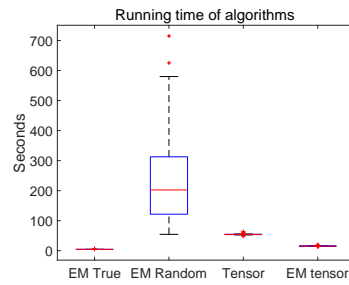


(c) Running time of the algorithms

Figure 19: $N = 10000, J = 200, L = 10$, item parameters $\in \{0.1, 0.2, 0.8, 0.9\}$

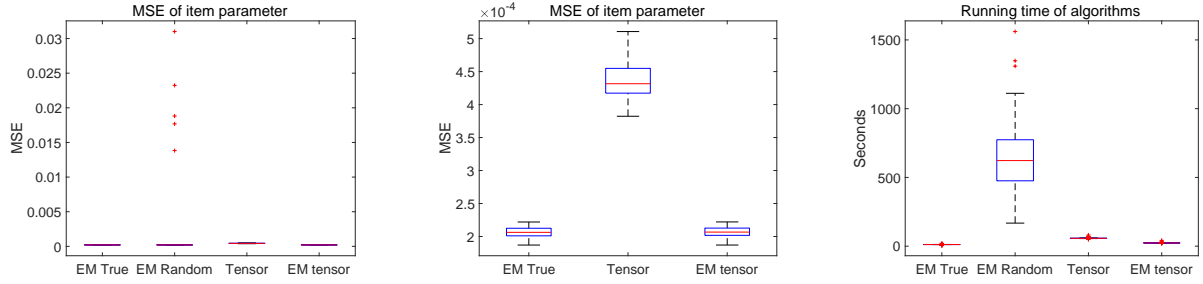


(a) MSE of item parameters



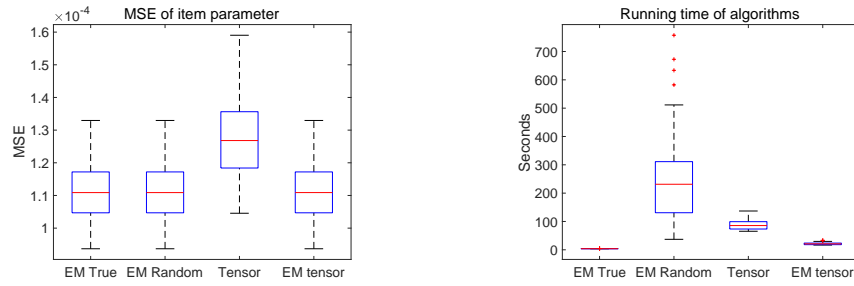
(b) Running time of the algorithms

Figure 20: $N = 10000, J = 100, L = 5$, item parameters $\in \{0.2, 0.4, 0.6, 0.8\}$



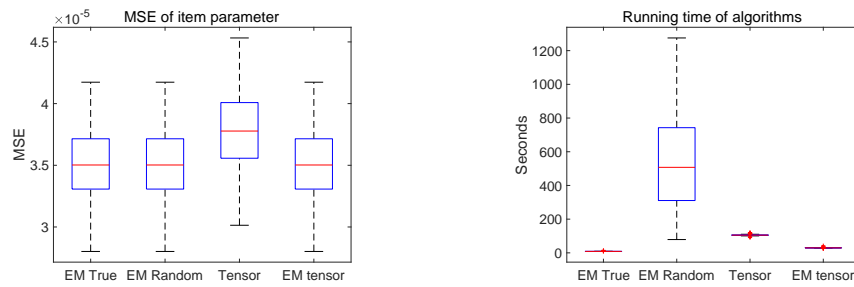
(a) MSE of item parameters (b) MSE without EM-random (c) Running time of the algorithms

Figure 21: $N = 10000, J = 100, L = 10$, item parameters $\in \{0.2, 0.4, 0.6, 0.8\}$



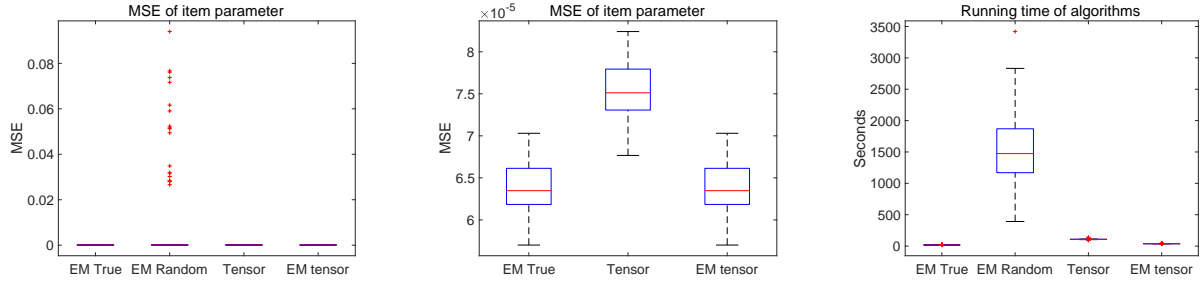
(a) MSE of item parameters (b) Running time of the algorithms

Figure 22: $N = 10000, J = 200, L = 5$, item parameters $\in \{0.2, 0.4, 0.6, 0.8\}$



(a) MSE of item parameters (b) Running time of the algorithms

Figure 23: $N = 20000, J = 100, L = 5$, item parameters $\in \{0.1, 0.2, 0.8, 0.9\}$

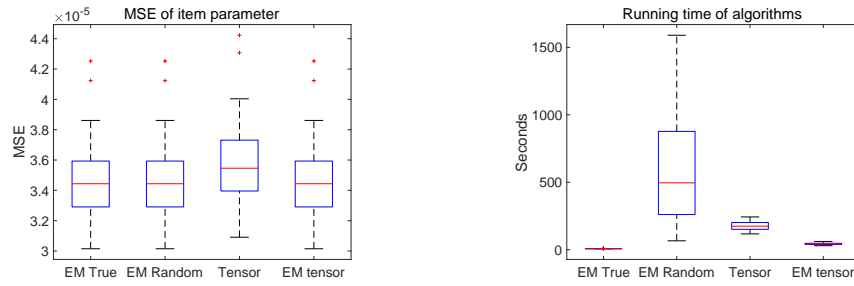


(a) MSE of item parameters

(b) MSE without EM-random

(c) Running time of the algorithms

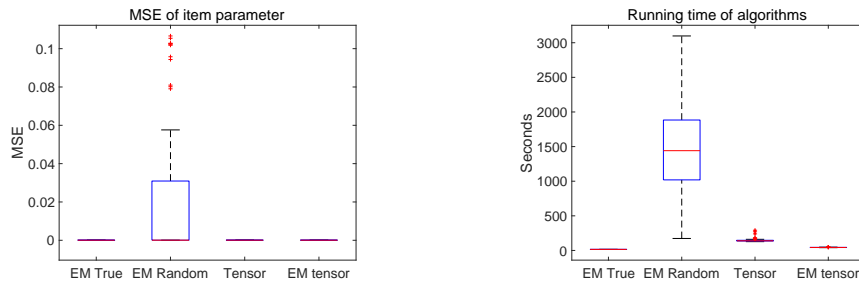
Figure 24: $N = 20000, J = 100, L = 10$, item parameters $\in \{0.1, 0.2, 0.8, 0.9\}$



(a) MSE of item parameters

(b) Running time of the algorithms

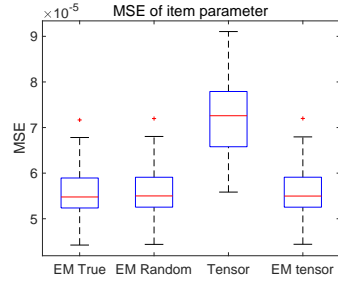
Figure 25: $N = 20000, J = 200, L = 5$, item parameters $\in \{0.1, 0.2, 0.8, 0.9\}$



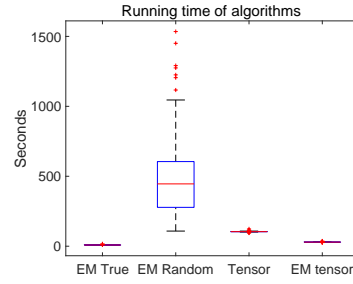
(a) MSE of item parameters

(b) Running time of the algorithms

Figure 26: $N = 20000, J = 200, L = 10$, item parameters $\in \{0.1, 0.2, 0.8, 0.9\}$

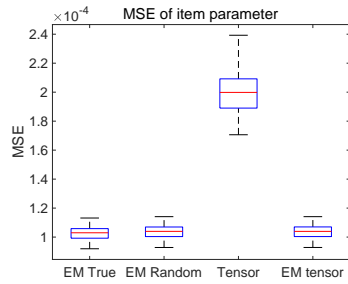


(a) MSE of item parameters

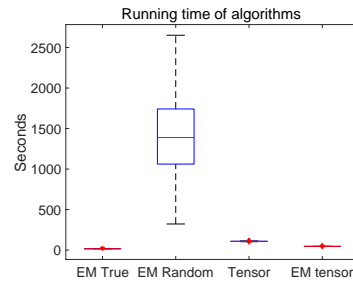


(b) Running time of the algorithms

Figure 27: $N = 20000, J = 100, L = 5$, item parameters $\in \{0.2, 0.4, 0.6, 0.8\}$

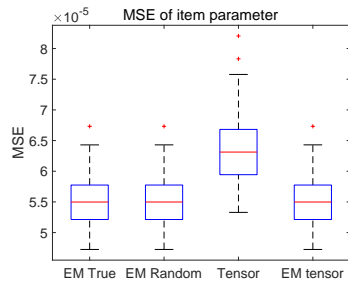


(a) MSE of item parameters

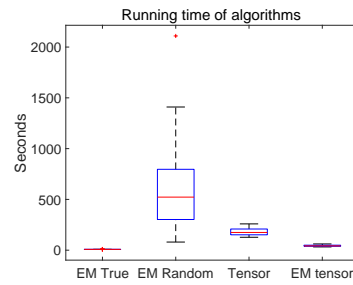


(b) Running time of the algorithms

Figure 28: $N = 20000, J = 100, L = 10$, item parameters $\in \{0.2, 0.4, 0.6, 0.8\}$

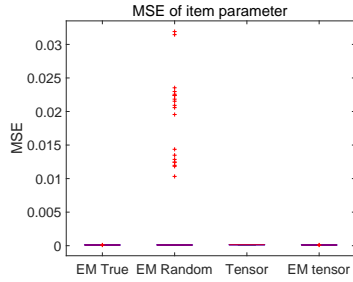


(a) MSE of item parameters

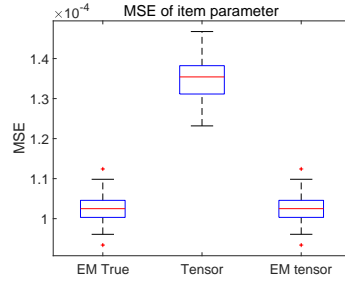


(b) Running time of the algorithms

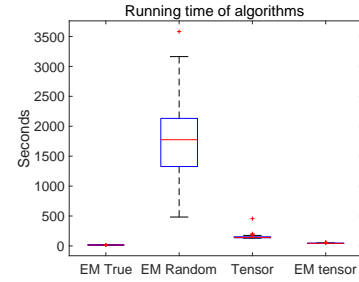
Figure 29: $N = 20000, J = 200, L = 5$, item parameters $\in \{0.2, 0.4, 0.6, 0.8\}$



(a) MSE of item parameters



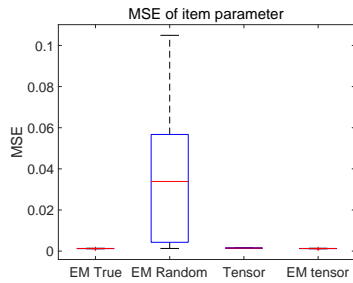
(b) MSE without EM-random



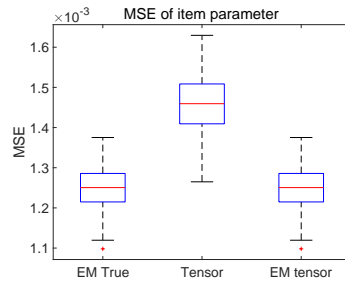
(c) Running time of the algorithms

Figure 30: $N = 20000, J = 200, L = 10$, item parameters $\in \{0.2, 0.4, 0.6, 0.8\}$

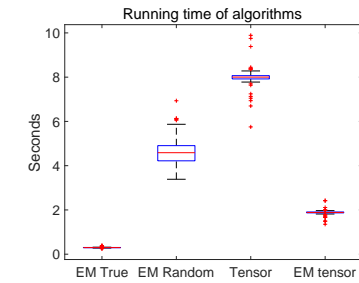
Then the simulation results of fixed-effect LCM are presented.



(a) MSE of item parameters

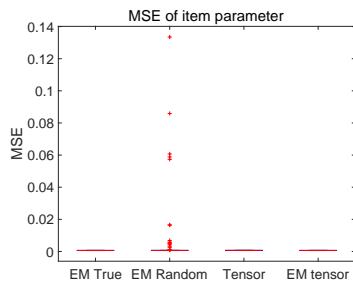


(b) MSE without EM-random

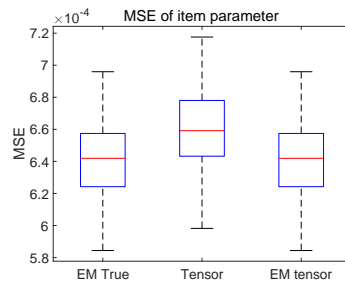


(c) Running time of the algorithms

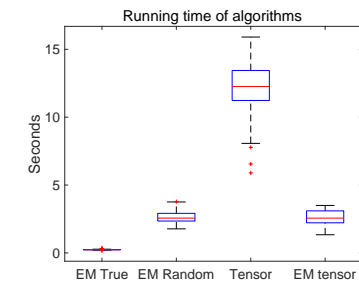
Figure 31: $N = 1000, J = 100, L = 10$, item parameters $\in \{0.1, 0.2, 0.8, 0.9\}$



(a) MSE of item parameters

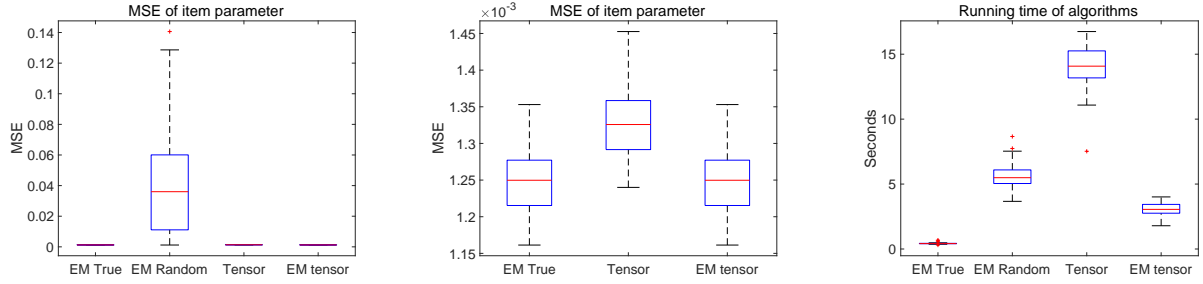


(b) MSE without EM-random



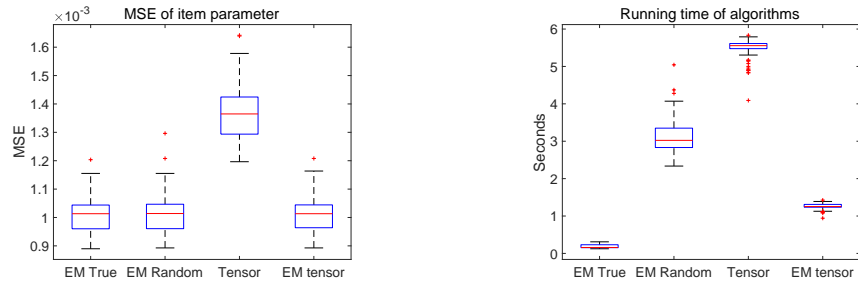
(c) Running time of the algorithms

Figure 32: $N = 1000, J = 200, L = 5$, item parameters $\in \{0.1, 0.2, 0.8, 0.9\}$



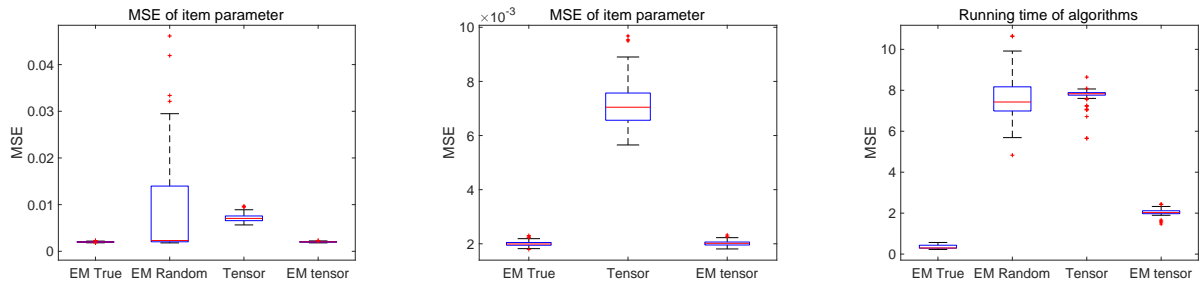
(a) MSE of item parameters (b) MSE without EM-random (c) Running time of the algorithms

Figure 33: $N = 1000, J = 200, L = 10$, item parameters $\in \{0.1, 0.2, 0.8, 0.9\}$



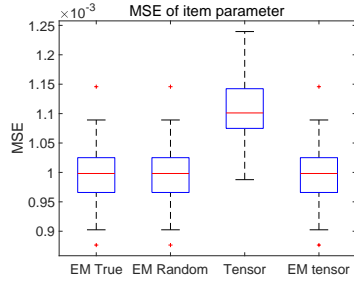
(a) MSE of item parameters (b) Running time of the algorithms

Figure 34: $N = 1000, J = 100, L = 5$, item parameters $\in \{0.2, 0.4, 0.6, 0.8\}$

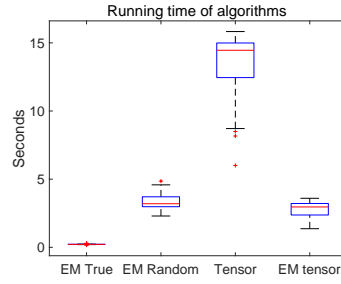


(a) MSE of item parameters (b) MSE without EM-random (c) Running time of the algorithms

Figure 35: $N = 1000, J = 100, L = 10$, item parameters $\in \{0.2, 0.4, 0.6, 0.8\}$

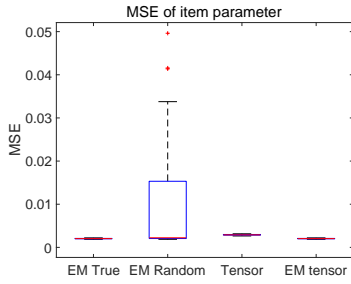


(a) MSE of item parameters

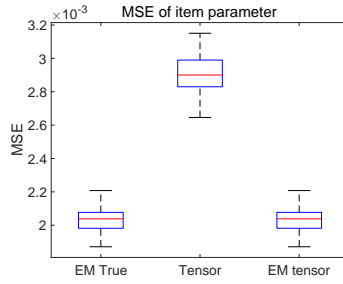


(b) Running time of the algorithms

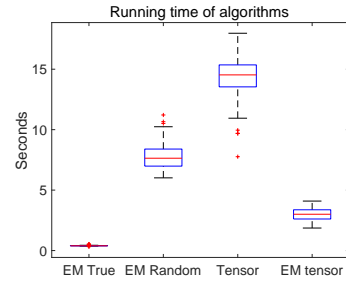
Figure 36: $N = 1000, J = 200, L = 5$, item parameters $\in \{0.2, 0.4, 0.6, 0.8\}$



(a) MSE of item parameters

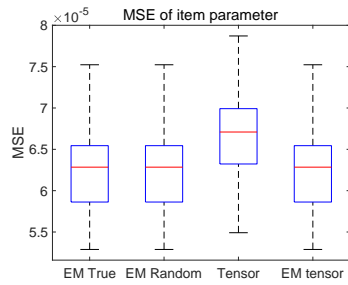


(b) MSE without EM-random

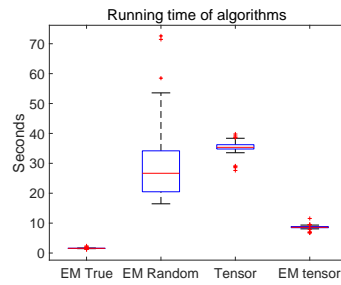


(c) Running time of the algorithms

Figure 37: $N = 1000, J = 200, L = 10$, item parameters $\in \{0.2, 0.4, 0.6, 0.8\}$

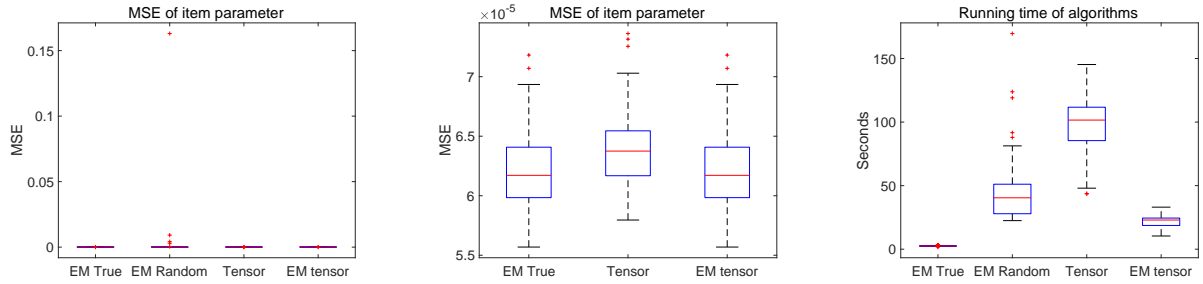


(a) MSE of item parameters



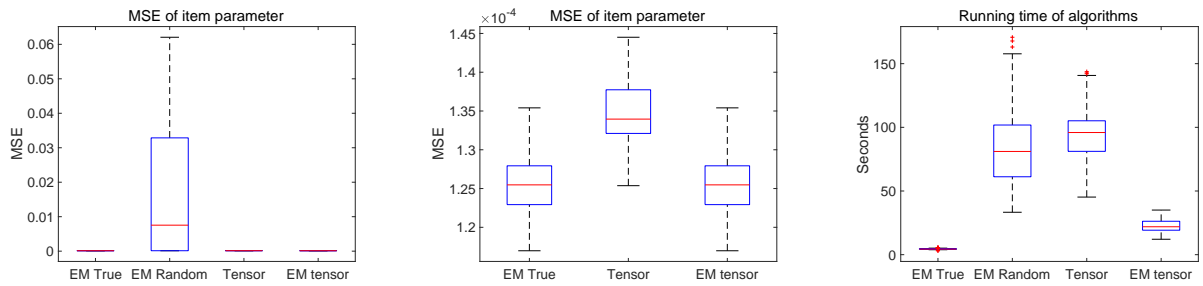
(b) Running time of the algorithms

Figure 38: $N = 10000, J = 100, L = 5$, item parameters $\in \{0.1, 0.2, 0.8, 0.9\}$



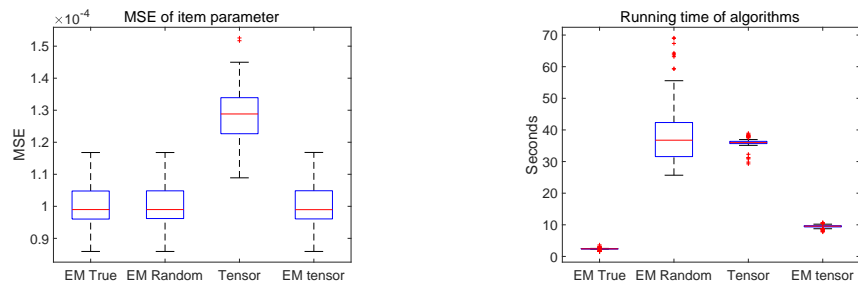
(a) MSE of item parameters (b) MSE without EM-random (c) Running time of the algorithms

Figure 39: $N = 10000, J = 200, L = 5$, item parameters $\in \{0.1, 0.2, 0.8, 0.9\}$



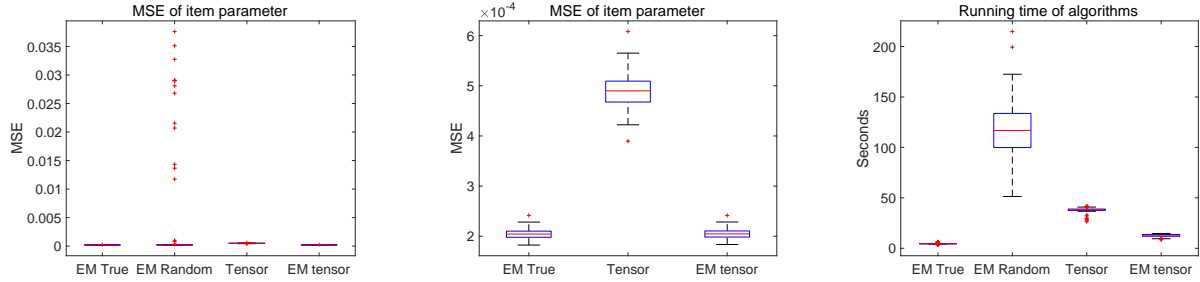
(a) MSE of item parameters (b) MSE without EM-random (c) Running time of the algorithms

Figure 40: $N = 10000, J = 200, L = 10$, item parameters $\in \{0.1, 0.2, 0.8, 0.9\}$



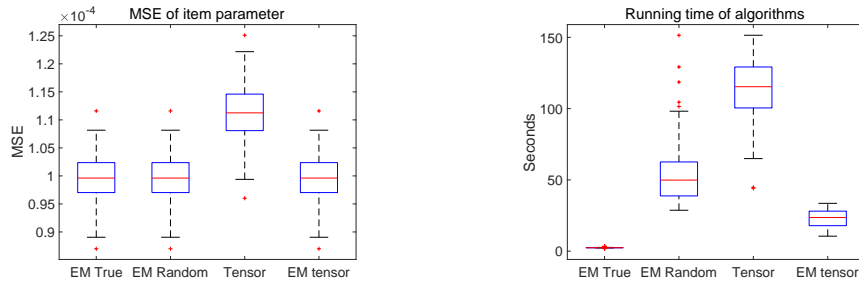
(a) MSE of item parameters (b) Running time of the algorithms

Figure 41: $N = 10000, J = 100, L = 5$, item parameters $\in \{0.2, 0.4, 0.6, 0.8\}$



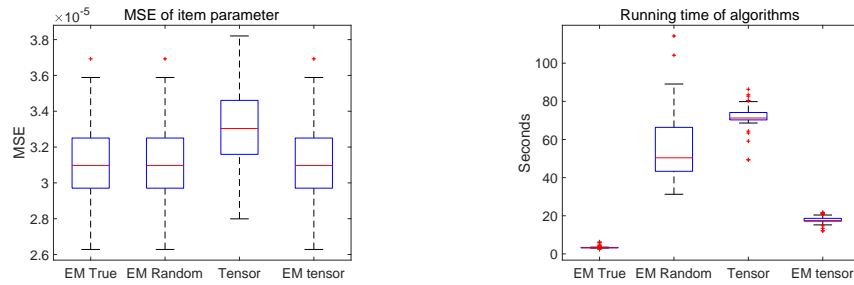
(a) MSE of item parameters (b) MSE without EM-random (c) Running time of the algorithms

Figure 42: $N = 10000, J = 100, L = 10$, item parameters $\in \{0.2, 0.4, 0.6, 0.8\}$



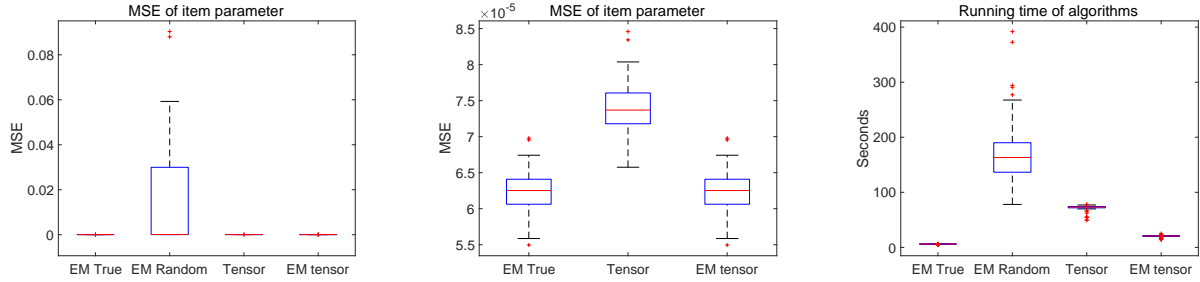
(a) MSE of item parameters (b) Running time of the algorithms

Figure 43: $N = 10000, J = 200, L = 5$, item parameters $\in \{0.2, 0.4, 0.6, 0.8\}$



(a) MSE of item parameters (b) Running time of the algorithms

Figure 44: $N = 20000, J = 100, L = 5$, item parameters $\in \{0.1, 0.2, 0.8, 0.9\}$

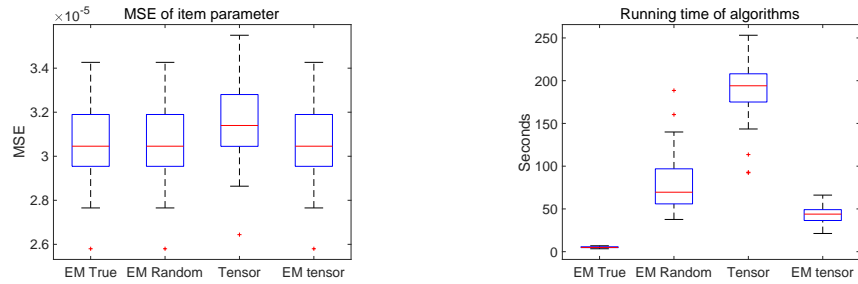


(a) MSE of item parameters

(b) MSE without EM-random

(c) MSE without EM-random

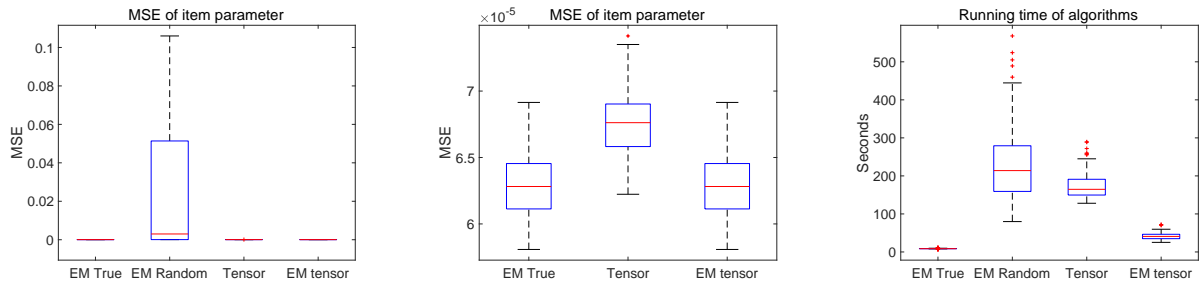
Figure 45: $N = 20000, J = 100, L = 10$, item parameters $\in \{0.1, 0.2, 0.8, 0.9\}$



(a) MSE of item parameters

(b) Running time of the algorithms

Figure 46: $N = 20000, J = 200, L = 5$, item parameters $\in \{0.1, 0.2, 0.8, 0.9\}$

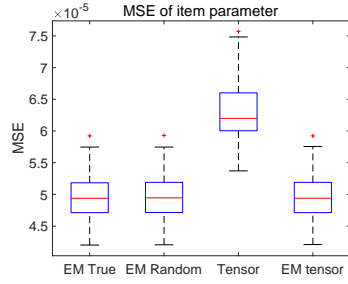


(a) MSE of item parameters

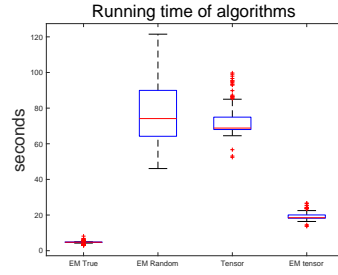
(b) MSE without EM-random

(c) Running time of the algorithms

Figure 47: $N = 20000, J = 200, L = 10$, item parameters $\in \{0.1, 0.2, 0.8, 0.9\}$

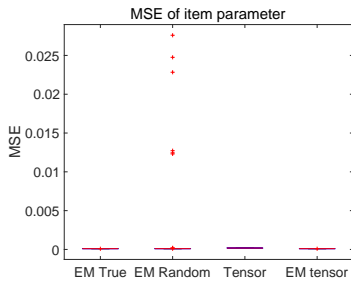


(a) MSE of item parameters

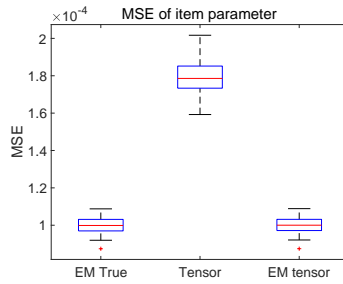


(b) Running time of the algorithms

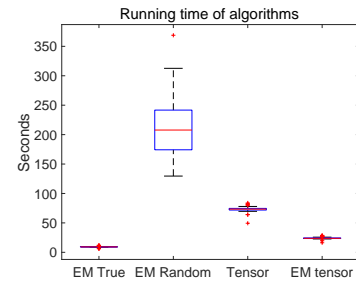
Figure 48: $N = 20000, J = 100, L = 5$, item parameters $\in \{0.2, 0.4, 0.6, 0.8\}$



(a) MSE of item parameters

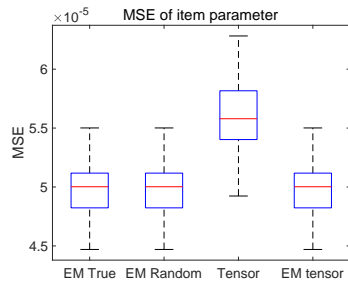


(b) MSE without EM-random

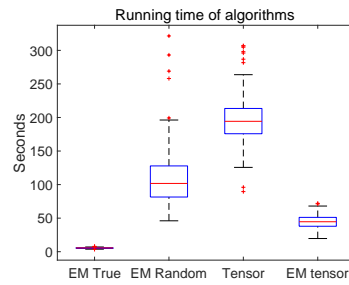


(c) Running time of the algorithms

Figure 49: $N = 20000, J = 100, L = 10$, item parameters $\in \{0.2, 0.4, 0.6, 0.8\}$

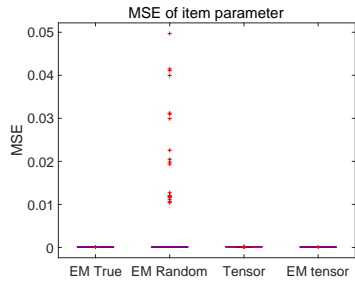


(a) MSE of item parameters

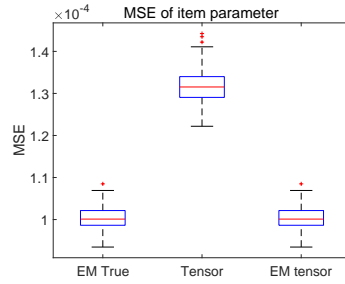


(b) Running time of the algorithms

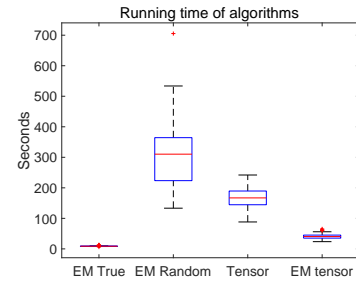
Figure 50: $N = 20000, J = 200, L = 5$, item parameters $\in \{0.2, 0.4, 0.6, 0.8\}$



(a) MSE of item parameters



(b) MSE without EM-random



(c) Running time of the algorithms

Figure 51: $N = 20000, J = 200, L = 10$, item parameters $\in \{0.2, 0.4, 0.6, 0.8\}$